

supporting information to:

Self-reporting styrylthiazolium photopharmaceuticals: mitochondrial localisation as well as SAR drive biological activity

Li Gao, Yvonne Kraus, Andrea Stegner, Thomas Wein, Constanze Heise, Leonie von Brunn, Elena Fajardo-Ruiz, Julia Thorn-Seshold, Oliver Thorn-Seshold*

Department of Pharmacy, Ludwig-Maximilians University Munich, 5-13 Butenandtstr., Munich 81377, Germany.

*correspondence to: oliver.thorn-seshold@cup.lmu.de; ORCID: OT-S: 0000-0003-3981-651X

Authorship Statement: LG designed targets, performed synthesis, chemical analysis, photocharacterisation, cell cytotoxicity studies, and wrote the manuscript. YK performed fixed and live cell imaging. AS and LvB performed synthesis. TW performed docking studies. CH performed cell cytotoxicity studies and transfections. EFR performed *in vitro* tubulin polymerisation. JTS supervised cellular assays and analysed biological data. OTS designed the study, designed targets, supervised chemistry and wrote the manuscript.

Table of Contents

Supporting Notes.....	2
Supporting Note 1: Performance of known photoswitchable colchicinoid inhibitors.....	2
Supporting Note 2: Summary of SBTub SAR as relevant to StyBtz/StyTz design.....	2
Supporting Note 3: Hypotheses for StyBtz structure-and-light-dependent action.....	3
Supporting Note 4: StyBtz constitution.....	4
Part A: Chemical Synthesis.....	4
Conventions.....	4
Standard Procedures.....	5
Experimental Data.....	7
Part B: Photocharacterisation in vitro.....	14
Spectrophotometry methods.....	14
Spontaneous relaxation.....	16
pH dependence of spontaneous relaxation rate.....	17
Solvent dependence of spontaneous relaxation.....	18
Fluorescence measurement.....	18
PSS measurements; comparison to calculated $\phi(\lambda)$; estimated $E(\lambda)$	19
Photosensitization assay.....	20
Part C: Biological and Biochemical Data.....	21
Cell culture and illuminations in cell culture.....	21
Resazurin antiproliferation assay.....	21
Immunofluorescence.....	22
Cell cycle analysis.....	23
Stability to glutathione.....	23
Tubulin polymerisation assay.....	24
Live cell imaging.....	24
Part D: Crystallographic Data.....	26
Part E: NMR Spectra.....	27
Supporting Information References.....	43

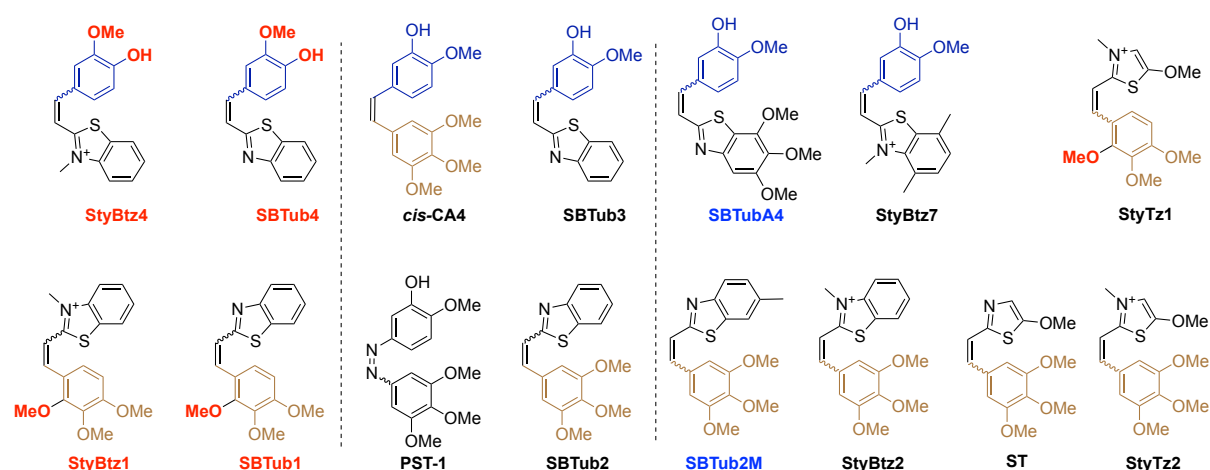
Supporting Notes

Supporting Note 1: Performance of known photoswitchable colchicinoid inhibitors

The photoswitchable tubulin inhibitors most extensively used in biology are azobenzene-based PSTs^[1] and heterostilbene-based SBTubs^[2], inspired by *cis*-active stilbene combretastatin A4 (CA4)^[3] (**Fig 1a**). While *E* → *Z* photoisomerization of the stilbene CA4 is technically possible, it requires <330 nm light and causes 6π-electrocyclisation-degradation: so preventing its biological application as a switch.^[4,5] Instead, azobenzene PSTs allow bidirectional photoswitching of MT dynamics in systems up to early embryos (*E* → *Z* around 405 nm, *Z* → *E* around 514 nm),^[6,7] and have been applied to help to resolve key questions in cellular and developmental biology^[8–10], despite the drawback that their *Z*-isomers are significantly degraded by cellular thiols^[2]. SBTubs are benzothiazole-based heterostilbene photopharmaceuticals^[2] with even better *E* → *Z* photoswitching at 405 nm, which were developed to deliver both metabolic robustness (photoswitch based on C=C rather than N=N) and optical transparency to GFP-imaging (ca. 488 nm) (**Fig 1b**). The cost of these improvements was sacrificing the possibility of bulk *Z* → *E* photoswitching; in turn, since SBTs are slow-relaxing on the biological timescale, this forces experimenters to rely on diffusion (which occurs on the seconds (cells) to minutes (tissues) timescale) to relieve the inhibition caused by *E* → *Z* photoswitching in a target area. Nonetheless, SBTubs have already succeeded across numerous *in vivo* applications.^[11]

Supporting Note 2: Summary of SBTub SAR as relevant to StyBtz/StyTz design

First-generation **SBTub2/3**^[2] were optimised by screening^[11].



Scheme S1 - Key SBT/ST/StyBtz/StyTz relevant to SAR predictions

SBTub2/3 bind tubulin as their *Z* isomers (**Fig 1b**); while regioisomers **SBTub1/4**'s displaced methoxy groups clash with SAR so they are not tubulin inhibitors, serving as mechanism controls^[2]. Therefore, considering the potency of the *Z* isomers:

(1) Because **SBTub2/3** and **ST** are tubulin binders, we were hopeful of similar bioactivity for their respective analogues **StyBtz2/3** and **StyTz2**.

(2) It is the "outer rim" methoxy group in **SBTub1** that kills potency, so we expected **StyBtz1** and **StyTz1** and **StyBtz5** to likewise be non-tubulin-binding controls. It is the placement of a larger less polar OMe at the 3-position instead of 4-position in **SBTub4** kills potency, so we expected similarly to find analogue **StyBtz4** inactive on tubulin.

(3) The methyl group of **SBTub2M** adds >10-fold potency compared to **SBTub2**: though the methyl is not tolerated at other positions, and replacing it with a methoxy group is also not tolerated: so we decided to test by docking and experiment if **StyBtz6/7** would tolerate their methylations compared to respective parent compounds **StyBtz2/3**.

Supporting Note 3: Hypotheses for StyBtz structure-and-light-dependent action

The possibilities with these reagents (*E/Z*-bioactivities and biolocalisations all differing between the methylated, vs demethylated, vs methylated but thiol-added Michael product, etc) are complex.

We believe that the acute cellular behaviour of StyBtz is driven by their accumulation into mitochondria; in which, under sufficiently high intensity illumination, they can structure-dependently cause either **(A) depolarisation** (e.g. deprotonatable **StyBtz4**, causing acute self-leakage to the cytosol in **Fig 4b**) and/or **(B) rupturing of mitochondrial membranes** (e.g. **StyBtz2**, **Fig 4a**, **Fig S12**) which both rapidly distributes the StyBtz to the cytosol, and also leaks mitochondrial machinery such as cytochromes which in turn causes acute blebbing and catastrophic cell death (**Fig S12a**).

Coherent with this picture, while this work was in preparation, Rivera-Fuentes reported structurally similar (though significantly more charge-delocalised) DLCs based on a *para*-amino-styrylindoleninium, that likewise concentrate in mitochondria and can be released to the cytosol upon depolarisation.^[12]

Also coherent with this picture, it appeared that biological disruption in **Fig 12c-d** propagates spatially within cells over a timescale of seconds following subcellular targeting: this matches small molecule diffusion speeds, but *not* that of the **StyBtz2**, which imaging showed is slower to spread; mitochondrial components (such as cytochromes) are potential candidates.

We assume it is more likely that the mitochondrial damage is caused by localised photothermal heating (dissipation of incoming photon energies into a small environment), rather than by acute photosensitisation (timescale too short) or by the microscopic motions of isomerisation^[13], although this question cannot easily be resolved.

It is entirely possible that StyTz / StyBtz which were nontoxic in the longterm cellular assays would have proved to be acutely phototoxic at high illumination intensities.

The longterm cellular behaviour of StyBtz at low light intensities and duty cycles (longterm cellular toxicity or microtubule network architecture assays) is more difficult to interpret. One possibility is that they do not act against mitochondria, but rather act as prodrugs of which some small proportion that escapes degradation by nucleophiles performing Michael addition (**Fig 3**) can instead be demethylated (by hydrolysis or other nucleophiles) to give the corresponding neutral STs or SBTs, that no longer remain localised to mitochondria but now perform *Z*-specific tubulin binding. In our experience, cell

cycle assays (20 h) give ca. 5-fold higher IC₅₀s with this class of inhibitors than do antiproliferation assays (48 h);^[1,2] and the different assay durations may also mean that more **SBTub2** is released in the antiproliferation assay; this may offer an explanation for why we did not see cell cycle arrest with lit **StyBtz2**, but did see MT disruption and antiproliferative effects.

Supporting Note 4: StyBtz constitution

The positive charge on StyBtz is plausible because their properties are self-similar within the group, while being significantly different from those of the neutral, non-alkylated SBT precursors: their UVVis-spectra have abs max around 450 nm (Fig S1-S2; for SBTs these are around 350 nm); *Z* → *E* relaxation times are in the minutes range (Fig S3; not >>24 h for neutral heterostilbenes); retention times on RP-HPLC are significantly shorter than those of the corresponding neutral, non-methylated, SBT precursors; mitochondrial localisation; etc. (ii) A crystal structure also resolves the *N*-methyl group and the iodide counterion, see [Table S1](#).

Part A: Chemical Synthesis

Conventions

Abbreviations: The following abbreviations are used: Hex – distilled isohexanes, EA – ethyl acetate, DCM – dichloromethane

Safety Hazards: no unexpected or unusually high safety hazards were encountered.

Reagents and Conditions: Unless stated otherwise, (1) all reactions and characterizations were performed with unpurified, undried, non-degassed solvents and reagents, used as obtained, under closed air atmosphere without special precautions; (2) “hexane” used for chromatography was distilled from commercial crude isohexane fraction by rotary evaporation; (3) “column” and “chromatography” refer to manual flash column chromatography on Merck silica gel Si-60 (40–63 μm); (4) procedures and yields are unoptimized; (5) yields refer to isolated chromatographically and spectroscopically pure materials, corrected for residual solvent content; (6) all eluent and solvent mixtures are given as volume ratios unless otherwise specified, thus “1:1 Hex:EA” indicates a 1:1 (v/v) mixture of hexanes and ethyl acetate; (7) chromatography eluents e.g. “0 → 25% EA:Hex” indicate a linear gradient of eluent composition.

Thin-layer chromatography (TLC) was run on 0.25 mm Merck silica gel plates (60, F-254), typically with Hex:EA eluents, except where indicated. UV light (254 nm) was used as a visualizing agent, with cross-checking by 365 nm UV lamp. TLC characterizations are abbreviated as $R_f = 0.64$ (EA:Hex = 1:1).

NMR: Standard NMR characterization was by ¹H- and ¹³C-NMR spectra on a Bruker Ascend 400 (400 MHz & 100 MHz for ¹H and ¹³C respectively) or a Bruker Ascend 500 (500 MHz & 100 MHz for ¹H and ¹³C respectively). Known compounds were checked against literature data and their spectral analysis is not detailed unless necessary. Chemical shifts (δ) are reported in ppm calibrated to residual

non-perdeuterated solvent as an internal reference^[14]. Peak descriptions singlet (s), doublet (d), triplet (t), quartet (q) and multiplet (m). All StyBtz NMRs are of all-*trans* populations.

Analytical HPLC and Mass Spectra: Analytical HPLC-MS measurements were performed on an Agilent 1100 SL coupled HPLC-MS system with (a) a binary pump to deliver H₂O:MeCN eluent mixtures containing 0.1% formic acid at a 0.4 mL/min flow rate, (b) Thermo Scientific Hypersil GOLD™ C18 column (1.9 μm; 3 × 50 mm) maintained at 22°C, whereby the solvent front eluted at $t_{ret} = 0.5$ min, (c) an Agilent 1100 series diode array detector used to acquire peak spectra of separated compounds/isomers in the range 200-550 nm after manually baselining across each elution peak of interest to correct for eluent composition effects, (d) a Bruker Daltonics HCT-Ultra mass spectrometer used in ESI mode at unit mass resolution. Run conditions were a linear gradient of H₂O:MeCN eluent composition from the starting ratio through to 10:90, applied during the separation phase (first 5 min), then 0:100 maintained until all peaks of interest had been observed (typically 2 min more); the column was equilibrated with the H₂O:MeCN eluent mixture for 2 minutes before each run. All reported peaks in the positive mode were [M+H]⁺ peaks. HRMS was carried out by the Zentrale Analytik of the LMU Munich using ESI or EI ionization as specified: Electron impact (EI) ionisation was performed on a Thermo Q Exactive GC Orbitrap or Finnigan MAT 95 sector field mass spectrometer. The resolution was set to approximately 5000 (MAT95) or 50 000 (at m/z 200, Q Exactive GC). Depending on the used method, a span from 40 to 1040 u was detected. Ionisation was performed at 250 °C source temperature and 70 eV electron energy. Electrospray ionisation (ESI) was performed on a Thermo Finnigan LTQ FT Ultra Fourier Transform Ion Cyclotron Resonance Spectrometer. The resolution was set to 100 000 at m/z 400. Depending on the used method, a span from 50 to 2000 u was detected. The current of the spray capillary at the IonMax ESI probe head was 4 kV, the temperature of the heating capillary 250 °C, N₂ flow of sheath gas 20 and the sweep gas flow 5 units.

Standard Procedures

Where Standard Procedures were used in synthesis, unless stated otherwise, the amounts of reactants/reagents employed were implicitly adjusted to maintain the same molar ratios as in the given Procedure, and no other alterations from the Standard Procedure (e.g. reaction time, extraction solvent, temperature) were made, unless stated otherwise.

Standard Procedure A: Styrylbenzothiazolium formation by condensation of *N*-methyl-benzothiazolium and benzaldehyde

Styrylbenzothiazolium salts were synthesized following a procedure by Coelho^[15]. To a mixture of benzothiazolium salt (1.0 eq) and benzaldehyde (1.0 eq) in ethanol (10 mL/mmol) were added piperidine (0.1 eq) and the reaction mixture was stirred for 6 h at reflux. After cooling down to room temperature the precipitate was filtered off and washed with cold ethyl acetate to give the styrylbenzothiazolium salts as amorphous powders.

Standard Procedure B: Styrylthiazolium formation by condensation of 2,3-dimethylthiazolium and benzaldehyde

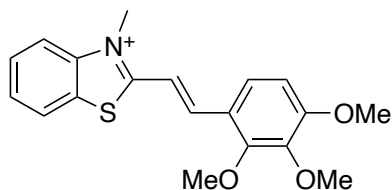
Styrylthiazolium iodide salts were synthesized from commercially available glycine methyl ester hydrochloride following a procedure by Tarbell^[16]. To a mixture of the thiazolium salt (1.0 eq) and benzaldehyde (1.0 eq) in ethanol (10 mL/eq) was added piperidine (0.1 eq) and the reaction mixture was stirred for 6 h at reflux. After cooling down to room temperature the precipitate was filtered off and washed with cold ethyl acetate to give the corresponding styrylthiazolium iodide salts as solids.

Standard Procedure C: Synthesis of N-methyl benzothiazolium salts

To a solution of 2-methylbenzothiazole derivative in MeCN (3 mL/mmol) was added methyl iodide (10 eq) and the reaction mixture was stirred for 16 h at 80°C. After cooling to room temperature the precipitate was filtered off and washed with cold ether to give the desired benzothiazolium iodide salt.

Experimental Data

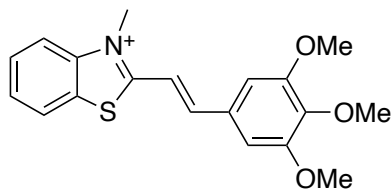
3-methyl-2-(2,3,4-trimethoxystyryl)benzothiazolium (StyBtz1)



Synthesised by Standard Procedure A, from 2,3-dimethylbenzothiazolium iodide **1** (582 mg, 2.0 mmol, 1.0 eq), 2,3,4-trimethoxybenzaldehyde (392 mg, 2.0 mmol, 1.0 eq) and piperidine (20 μ L, 0.20 mmol, 0.1 eq) in 20 mL EtOH. **StyBtz1** iodide (768 mg, 1.64 mmol, 82%) was obtained as an orange powder.

¹H-NMR (400 MHz, *d*₆-DMSO): δ = 8.39 (d, *J* = 8.1 Hz, 1H), 8.24 (d, *J* = 8.3 Hz, 1H), 8.09 (d, *J* = 16.0 Hz, 1H), 7.98 (d, *J* = 9.0 Hz, 1H), 7.93 (d, *J* = 15.9 Hz, 1H), 7.86 (ddd, *J* = 8.5, 7.3, 1.3 Hz, 1H), 7.77 (ddd, *J* = 8.3, 7.2, 1.0 Hz, 1H), 7.05 (d, *J* = 9.0 Hz, 1H), 4.33 (s, 3H), 3.98 (s, 3H), 3.93 (s, 3H), 3.80 (s, 3H) ppm. **¹³C-NMR (100 MHz, *d*₆-DMSO):** δ = 172.2, 157.6, 153.4, 142.6, 142.0, 141.5, 129.3, 128.2, 127.4, 125.1, 124.1, 120.2, 116.7, 112.1, 108.8, 61.9, 60.6, 56.4, 36.3 ppm. **HRMS (ESI, positive):** 342.11584 calculated for C₁₉H₂₀NO₃S⁺ [M]⁺, 342.11572 found.

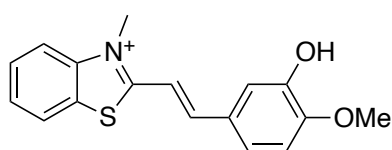
3-methyl-2-(3,4,5-trimethoxystyryl)benzothiazolium (StyBtz2)



Synthesised by Standard Procedure A, from 2,3-dimethylbenzothiazolium iodide **1** (500 mg, 1.72 mmol, 1.0 eq), 3,4,5-trimethoxybenzaldehyde (337 mg, 1.72 mmol, 1.0 eq) and piperidine (17 μ L, 0.172 mmol, 0.1 eq) in 17 mL ethanol. **StyBtz2** iodide (714 mg, 1.52 mmol, 89%) was obtained as a brown powder. **StyBtz2** iodide was crystallized as monohydrate (see Part D for crystallographic data).

¹H-NMR (400 MHz, *d*₆-DMSO): δ = 8.46 (ddd, *J* = 8.0, 1.3, 0.5 Hz, 1H), 8.26 (dt, *J* = 8.5, 0.9 Hz, 1H), 8.17 (d, *J* = 15.8 Hz, 1H), 7.97 (d, *J* = 15.9 Hz, 1H), 7.88 (ddd, *J* = 8.5, 7.3, 1.3 Hz, 1H), 7.80 (ddd, *J* = 8.2, 7.2, 1.0 Hz, 1H), 7.43 (s, 2H), 4.43 – 4.35 (m, 3H), 3.91 (s, 6H), 3.78 (s, 3H) ppm. **¹³C-NMR (100 MHz, *d*₆-DMSO):** δ = 171.9, 153.2, 148.8, 142.1, 141.3, 129.4, 129.4, 128.4, 127.7, 124.3, 116.9, 113.0, 107.6, 60.3, 56.4, 36.6 ppm. **HRMS (ESI, positive):** 342.11584 calculated for C₁₉H₂₀NO₃S⁺ [M]⁺, 342.11573 found.

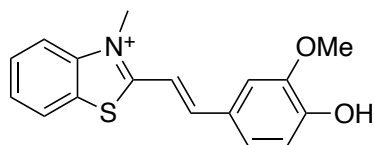
2-(3-hydroxy-4-methoxystyryl)-3-methylbenzothiazolium (StyBtz3)



Synthesised by Standard Procedure A, from 2,3-dimethylbenzothiazolium iodide **1** (582 mg, 2.0 mmol, 1.0 eq), 3-hydroxy-4-methoxybenzaldehyde (304 mg, 2.0 mmol, 1.0 eq) and piperidine (20 μ L, 0.20 mmol, 0.1 eq) in 20 mL ethanol. **StyBtz3** iodide (691 mg, 1.62 mmol, 81%) was obtained as an orange powder.

$^1\text{H-NMR}$ (400 MHz, d_6 -DMSO): δ = 9.35 (s, 1H), 8.40 (d, J = 8.8 Hz, 1H), 8.21 (d, J = 8.4 Hz, 1H), 8.09 (d, J = 15.7 Hz, 1H), 7.84 (t, J = 8.5 Hz, 1H), 7.78 (d, J = 15.8 Hz, 1H), 7.76 (t, J = 8.2 Hz, 1H), 7.56 – 7.48 (m, 2H), 7.10 (d, J = 9.0 Hz, 1H), 4.32 (s, 3H), 3.89 (s, 3H) ppm. **$^{13}\text{C-NMR}$ (100 MHz, d_6 -DMSO):** δ = 171.9, 152.1, 149.2, 146.8, 141.9, 129.2, 128.1, 127.5, 127.1, 124.1, 116.6, 115.5, 112.0, 111.1, 55.9, 36.2 ppm. **HRMS (ESI, positive):** 298.08963 calculated for $\text{C}_{17}\text{H}_{16}\text{NO}_2\text{S}^+$ $[\text{M}]^+$, 298.08951 found.

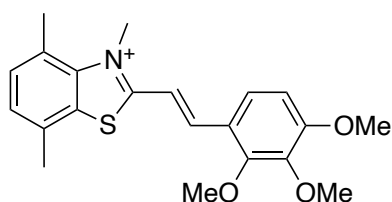
2-(4-hydroxy-3-methoxystyryl)-3-methylbenzothiazolium (StyBtz4)^[17]



Synthesised by Standard Procedure A, from 2,3-dimethylbenzothiazolium iodide **1** (582 mg, 2.0 mmol, 1.0 eq), 4-hydroxy-3-methoxybenzaldehyde (304 mg, 2.0 mmol, 1.0 eq) and piperidine (20 μ L, 0.20 mmol, 0.1 eq) in 20 mL ethanol. Known **StyBtz4** iodide (597 mg, 1.40 mmol, 70%) was obtained as a brown powder whose spectra match literature data.^[17]

$^1\text{H-NMR}$ (400 MHz, d_6 -DMSO): δ = 10.27 (s, 1H), 8.39 (d, J = 8.8 Hz, 1H), 8.20 (d, J = 8.4 Hz, 1H), 8.13 (d, J = 15.6 Hz, 1H), 7.85 (t, J = 8.5 Hz, 1H), 7.82 (d, J = 15.6 Hz, 1H), 7.76 (t, J = 8.2 Hz, 1H), 7.68 (d, J = 2.0 Hz, 1H), 7.54 (dd, J = 8.4, 2.0 Hz, 1H), 6.93 (d, J = 8.2 Hz, 1H), 4.33 (s, 3H), 3.91 (s, 3H) ppm. **$^{13}\text{C-NMR}$ (100 MHz, d_6 -DMSO):** δ = 172.1, 152.0, 149.6, 148.3, 142.0, 129.2, 128.0, 127.4, 126.2, 125.8, 124.1, 116.5, 115.9, 112.5, 110.1, 56.1, 36.2 ppm. **HRMS (ESI, positive):** 298.08963 calculated for $\text{C}_{17}\text{H}_{16}\text{NO}_2\text{S}^+$ $[\text{M}]^+$, 298.08951 found.

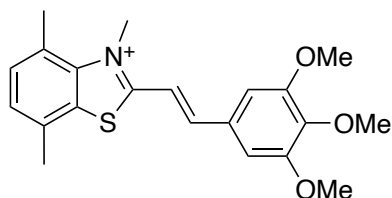
3,4,7-trimethyl-2-(2,3,4-trimethoxystyryl)benzothiazolium (StyBtz5)



Synthesised by Standard Procedure A, from 2,3,4,7-tetramethylbenzothiazolium iodide **5** (319 mg, 1.0 mmol, 1.0 eq), 2,3,4-trimethoxybenzaldehyde (196 mg, 1.0 mmol, 1.0 eq) and piperidine (9.88 μ L, 0.1 mmol, 0.1 eq) in 10 mL ethanol. **StyBtz5** iodide (192 mg, 0.386 mmol, 39%) was obtained as orange needles.

¹H-NMR (400 MHz, *d*₆-DMSO): δ = 8.13 (d, *J* = 15.8 Hz, 1H), 7.99 (d, *J* = 9.0 Hz, 1H), 7.94 (d, *J* = 15.8 Hz, 1H), 7.55 (dd, *J* = 7.5, 0.9 Hz, 1H), 7.48 (dd, *J* = 7.5, 0.9 Hz, 1H), 7.05 (d, *J* = 9.0 Hz, 1H), 4.52 (s, 3H), 3.98 (s, 3H), 3.93 (s, 3H), 3.80 (s, 3H), 2.91 (s, 3H), 2.59 (s, 3H) ppm. **¹³C-NMR (100 MHz, *d*₆-DMSO):** δ = 207.0, 171.7, 158.1, 154.0, 143.3, 142.0, 141.2, 133.9, 131.2, 128.9, 126.4, 125.6, 120.8, 112.7, 109.3, 62.5, 61.1, 56.9, 31.2, 21.0, 19.5 ppm. **HRMS (ESI, positive):** 370.14714 calculated for C₂₁H₂₄NO₃S⁺ [M]⁺, 370.14693 found.

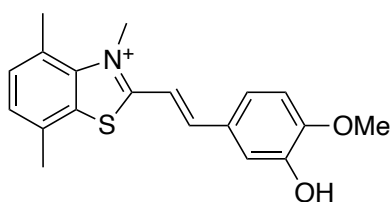
3,4,7-trimethyl-2-(3,4,5-trimethoxystyryl)benzothiazolium (StyBtz6)



Synthesised by Standard Procedure A, from 2,3,4,7-tetramethylbenzothiazolium iodide **5** (80 mg, 0.25 mmol, 1.0 eq), 3,4,5-trimethoxybenzaldehyde (49 mg, 0.25 mmol, 1.0 eq) and piperidine (2.5 μ L, 25 μ mol, 0.1 eq) in 2.5 mL ethanol. **StyBtz6** iodide (50 mg, 0.10 mmol, 40%) was obtained as an orange powder.

¹H-NMR (400 MHz, *d*₆-DMSO): δ = 8.22 (d, *J* = 15.7 Hz, 1H), 8.06 (d, *J* = 15.7 Hz, 1H), 7.55 (d, *J* = 7.6 Hz, 1H), 7.50 (d, *J* = 7.5 Hz, 1H), 7.44 (s, 2H), 4.59 (s, 3H), 3.90 (s, 6H), 3.77 (s, 3H), 2.93 (s, 3H), 2.58 (s, 3H) ppm. **¹³C-NMR (100 MHz, *d*₆-DMSO):** δ = 171.2, 153.2, 149.4, 141.3, 140.7, 133.4, 130.6, 129.5, 128.6, 128.4, 126.2, 113.1, 107.7, 60.3, 56.3, 39.9, 20.5, 18.9 ppm. **HRMS (ESI, positive):** 370.14714 calculated for C₂₁H₂₄NO₃S⁺ [M]⁺, 370.14711 found.

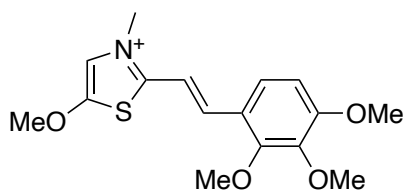
2-(3-hydroxy-4-methoxystyryl)-3,4,7-trimethylbenzothiazolium (StyBtz7)



Synthesised by Standard Procedure A, from 2,3,4,7-tetramethylbenzothiazolium iodide **5** (81 mg, 0.25 mmol, 1.0 eq), 4-hydroxy-3,5-dimethylbenzaldehyde (39 mg, 0.25 mmol, 1.0 eq) and piperidine (2.5 μ L, 25 μ mol, 0.1 eq) in 4.2 mL ethanol. **StyBtz7** iodide (46 mg, 0.10 mmol, 40%) was obtained as an orange powder.

¹H-NMR (400 MHz, *d*₆-DMSO): δ = 8.51 (s, 1H), 7.25 (d, *J* = 15.6 Hz, 1H), 6.92 (d, *J* = 15.6 Hz, 1H), 6.65 – 6.56 (m, 4H), 6.19 (d, *J* = 8.4 Hz, 1H), 3.62 (s, 3H), 2.99 (s, 3H), 2.01 (s, 3H), 1.68 (s, 3H) ppm. **¹³C-NMR (100 MHz, *d*₆-DMSO):** δ = 171.1, 152.1, 149.6, 146.9, 140.6, 133.3, 130.6, 128.4, 128.2, 127.2, 125.9, 124.1, 115.5, 112.0, 111.1, 55.9, 39.9, 20.6, 19.1 ppm. **HRMS (ESI, positive):** 326.12093 calculated for C₁₉H₂₀NO₂S⁺ [M+H]⁺, 326.12063 found.

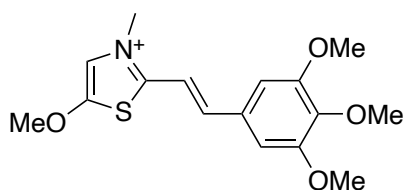
5-methoxy-3-methyl-2-(2,3,4-trimethoxystyryl)thiazolium (StyTz1)



Synthesised by Standard Procedure B, from 5-methoxy-2,3-dimethylthiazolium iodide **8** (144 mg, 0.531 mmol, 1.0 eq), 4-hydroxy-3,5-dimethylbenzaldehyde (208 mg, 1.06 mmol, 2.0 eq) and piperidine (52.4 μ L, 0.531 mmol, 1.0 eq) in 2 mL ethanol. **StyTz1** iodide (40 mg, 0.089 mmol, 17%) was obtained as a yellow powder.

¹H-NMR (400 MHz, *d*₆-DMSO): δ = 7.94 (s, 1H), 7.75 (d, *J* = 8.9 Hz, 1H), 7.64 (d, *J* = 16.0 Hz, 1H), 7.58 (d, *J* = 16.0 Hz, 1H), 7.00 (d, *J* = 9.0 Hz, 1H), 4.08 (s, 3H), 4.06 (s, 3H), 3.91 (s, 3H), 3.90 (s, 3H), 3.78 (s, 3H) ppm. **¹³C-NMR (100 MHz, *d*₆-DMSO):** δ = 158.5, 158.2, 156.5, 152.9, 141.6, 137.3, 124.3, 120.4, 117.8, 111.8, 108.6, 62.7, 61.7, 60.5, 56.2, 39.4 ppm. **HRMS (ESI, positive):** 322.11076 calculated for C₁₆H₂₀NO₄S⁺ [M]⁺, 322.11074 found.

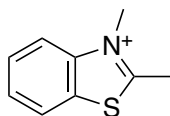
5-methoxy-3-methyl-2-(3,4,5-trimethoxystyryl)thiazolium (StyTz2)



Synthesised by Standard Procedure C, from 5-methoxy-2,3-dimethylthiazolium iodide **8** (144 mg, 0.531 mmol, 1.0 eq), 4-hydroxy-3,5-dimethylbenzaldehyde (208 mg, 1.06 mmol, 2.0 eq) and piperidine (52.4 μ L, 0.531 mmol, 1.0 eq) in 2 mL ethanol. **StyTz2** iodide (56 mg, 0.125 mmol, 23%) was obtained as an orange powder.

$^1\text{H-NMR}$ (400 MHz, d_6 -DMSO): δ = 7.97 (s, 1H), 7.71 (d, J = 15.9 Hz, 1H), 7.62 (d, J = 15.9 Hz, 1H), 7.23 (s, 2H), 4.11 (s, 3H), 4.08 (s, 3H), 3.86 (s, 6H), 3.73 (s, 3H) ppm. **$^{13}\text{C-NMR}$ (100 MHz, d_6 -DMSO):** δ = 158.8, 157.9, 153.2, 143.3, 140.4, 129.6, 117.9, 112.4, 106.6, 62.7, 60.2, 56.2, 39.7 ppm. **HRMS (ESI, positive):** 322.11076 calculated for $\text{C}_{16}\text{H}_{20}\text{NO}_4\text{S}^+$ [M] $^+$, 322.11070 found.

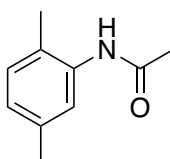
2,3-dimethylbenzothiazolium iodide (1)



To a solution of 2-methylbenzothiazole (3.0 g, 20 mmol, 1.0 eq) in 60 mL MeCN was added methyl iodide (1.9 mL, 30 mmol, 1.5 eq). The reaction mixture was stirred for 16 hours at reflux. After cooling to room temperature the precipitate was filtered off and washed with cold ether to give the desired known benzothiazolium iodide **1** as colorless crystals (4.35 g, 15 mmol, 74%) with spectra matching literature data.^[18]

$^1\text{H-NMR}$ (400 MHz, d_6 -DMSO): δ = 8.46 (d, J = 8.2 Hz, 1H), 8.30 (d, J = 8.4 Hz, 1H), 7.89 (t, J = 8.5 Hz, 1H), 7.80 (t, J = 8.2 Hz, 1H), 4.21 (s, 3H), 3.19 (s, 3H) ppm. **$^{13}\text{C-NMR}$ (100 MHz, d_6 -DMSO):** δ = 177.2, 141.5, 129.2, 128.7, 128.0, 124.5, 116.7, 36.3, 17.3 ppm. **HRMS (ESI, positive):** 164.05285 calculated for $\text{C}_9\text{H}_{10}\text{NS}^+$ [M] $^+$, 164.05275 found.

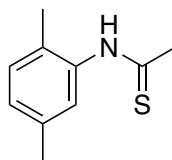
N-(2,5-dimethylphenyl)acetamide (2)



Acetic anhydride (11 g, 11 mmol, 1.2 eq) was added slowly to a solution of 2,5-dimethylaniline (1.1 g, 9.1 mmol, 1.0 eq) in DCM (15 mL) in a 50 mL flask. The reaction mixture was stirred for 1 h at room temperature and monitored by TLC. After completion, the mixture was quenched with a saturated aqueous solution of NaHCO₃ (25 mL). The organic layer was dried over MgSO₄, filtrated and the solvent was removed under reduced pressure to yield known *N*-(2,5-dimethylphenyl)acetamide **2** (1.35 g, 8.3 mmol, 90%) as a colorless powder, with spectra matching literature data.^[19]

¹H-NMR (400 MHz, CDCl₃): δ = 7.53 (s, 1H), 7.12 (s, 1H), 7.05 (d, J = 7.6 Hz, 1H), 6.89 (d, J = 7.6 Hz, 1H), 2.30 (s, 3H), 2.19 (s, 3H), 2.18 (s, 3H) ppm. **¹³C-NMR (100 MHz, CDCl₃):** δ = 168.6, 136.5, 135.4, 130.3, 126.6, 126.3, 124.3, 24.3, 21.2, 17.5 ppm. **R_f** = 0.35 (EA:Hex = 1:1). **HRMS (ESI, positive):** 164.10754 calculated for C₁₀H₁₄NO⁺ [M+H]⁺, 164.10700 found.

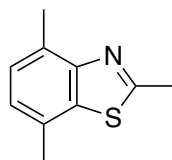
N-(2,5-dimethylphenyl)ethanethioamide (3)



N-(2,5-dimethylphenyl)acetamide **2** (812 mg, 4.97 mmol, 1.0 eq) was dissolved in THF (15 mL) and Lawessons's Reagent (2.5 g, 6.15 mmol, 1.24 eq) was added to the stirring solution. stirring. The reaction mixture was stirred for 2 h at reflux before cooling down to room temperature. Water (10 mL) was added and the suspension was extracted with EA (3 × 30 mL). The combined organic layers were washed with brine (30 mL), dried over Na₂SO₄, filtrated and concentrated *in vacuo* before filtering through a silica plug (EA:Hex = 1:10) to give crude *N*-(2,5-dimethylphenyl)ethanethioamide **3** (835 mg) with moderate purity that was used without further purification.

R_f = 0.76 (EA:Hex = 1:1). **HRMS (ESI, positive):** 180.08470 calculated for C₁₀H₁₄NS⁺ [M+H]⁺, 180.08407 found.

2,4,7-trimethylbenzothiazole (4)

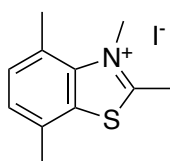


N-(2,5-dimethylphenyl)ethanethioamide **3** (1.31 g, 7.31 mmol, 1.0 eq) was dissolved in MeOH (9 mL) and 2 M NaOH (30 mL) was added. The reaction mixture was stirred at room temperature for 2 h. A solution of K₃[Fe(CN)₆] (7.2 g, 22 mmol, 3.0 eq) in H₂O (12 mL) was added at 0°C. The reaction mixture was warmed up to room temperature and stirring was continued for 3 h. The suspension was extracted

with EA (3 × 50 mL) and washed with brine (50 mL). The combined organic layers were dried over Na₂SO₄, filtrated and concentrated *in vacuo*. Column chromatography purification on silica gel (EA:Hex = 1:20) gave known 2,4,7-trimethylbenzothiazole **4** as a slightly yellowish oil (0.597 g, 3.4 mmol, 46%) with spectra matching literature data.^[11]

¹H-NMR (400 MHz, CDCl₃): δ = 7.18 (d, *J* = 7.4 Hz, 1H), 7.06 (d, *J* = 7.4 Hz, 1H), 2.89 (s, 3H), 2.71 (s, 3H), 2.49 (s, 3H) ppm. **¹³C-NMR (100 MHz, CDCl₃):** δ = 165.2, 152.1, 135.7, 129.2, 128.5, 126.5, 124.5, 21.2, 20.1, 18.1 ppm. **R_f** = 0.5 (EA:Hex = 1:20). **HRMS (EI, positive):** 177.0612 calculated for C₁₀H₁₁NS [M]⁺, 177.0603 found.

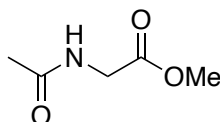
2,3,4,7-tetramethylbenzothiazolium (5)



2,4,7-trimethylbenzothiazole **4** (0.597 g, 3.4 mmol, 1.0 eq) was dissolved in MeCN (3 mL) and methyl iodide (1.3 mL, 20 mmol, 6.0 eq) was added. The reaction mixture was stirred overnight under reflux. After cooling to room temperature, THF, hexane and EA were added until no more precipitation was seen. The precipitate was filtered and washed with cold THF, giving **5** iodide salt as a colorless powder (126 mg, 0.395 mmol, 12%).

¹H-NMR (400 MHz, d₆-DMSO): δ = 7.58 (d, *J* = 7.6 Hz, 1H), 7.50 (d, *J* = 7.6 Hz, 1H), 4.39 (s, 3H), 3.19 (s, 3H), 2.90 (s, 3H), 2.58 (s, 3H) ppm. **¹³C-NMR (100 MHz, d₆-DMSO):** δ = 175.4, 140.2, 133.2, 130.9, 129.4, 128.0, 125.8, 40.0, 20.1, 18.9, 17.9 ppm. **HRMS (ESI, positive):** 192.08415 calculated for C₁₁H₁₄NS⁺ [M]⁺, 192.08410 found.

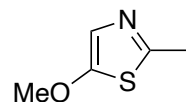
N-acetylglycine methyl ester (6)



N-acetylglycine methyl ester **6** was synthesized following a procedure by A. Padwa et al.³ To a stirred solution of glycine methyl ester hydrochloride (30 g, 24 mmol, 1.0 eq) in 200 mL chloroform was added triethylamine (73 mL, 53 mmol, 2.2 eq) at 0°C. The solution was allowed to stir at room temperature for 30 min before dropwise addition of acetyl chloride (19 mL, 26 mmol, 1.1 eq). After stirring another 3 h at room temperature the solvent was removed and redissolved in EA and filtered through a silica plug. After removing all volatiles, known N-acetylglycine methyl ester **6** was obtained as yellow oil, which solidified overnight (30 g, 23 mmol, 96%) with spectra matching literature data.^[20]

¹H-NMR (500 MHz, CDCl₃): δ = 6.88 (s, 1H), 3.89 (s, 2H), 3.62 (s, 3H), 1.92 (s, 3H) ppm. **¹³C-NMR (125 MHz, CDCl₃):** δ = 170.8, 170.5, 52.1, 41.1, 22.5 ppm. **R_f** = 0.15 (EA:Hex = 1:1). **HRMS (EI, positive):** 131.0582 calculated for C₅H₉NO₃ [M]⁺, 131.0576 found.

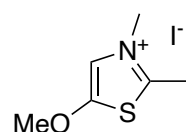
5-methoxy-2-methylthiazole (7)



5-methoxy-2-methylthiazole **7** was synthesized from N-acetylglycine methyl ester **6** (5.7 g, 43.5 mmol) following a procedure by Tarbell et al.^[16] to yield 1.09 g (8.45 mmol, 19%) of known 5-methoxy-2-methylthiazole, matching their spectral data^[16].

¹H-NMR (400 MHz, CDCl₃): δ = 6.85 (s, 1H), 3.86 (s, 3H), 2.54 (s, 3H) ppm. **¹³C-NMR (100 MHz, CDCl₃):** δ = 162.1, 153.9, 120.1, 61.5, 19.9 ppm. **R_f** = 0.52 (EA:Hex = 1:1). **HRMS (ESI, positive):** 130.03211 calculated for C₅H₈NOS⁺ [M+H]⁺, 130.03212 found.

5-methoxy-2,3-dimethylthiazolium iodide (8)



5-methoxy-2-methylthiazole **7** (645 mg, 5.0 mmol, 1.0 eq) was dissolved in 5 mL ethanol and methyl iodide (0.94 mL, 15 mmol, 3.0 eq) was added. The reaction mixture was refluxed overnight before cooling down to room temperature. The precipitate was filtered off and washed with cold ether to give 400 mg of the thiazolium iodide as colorless crystals (2.8 mmol, 56%).

¹H-NMR (500 MHz, d₆-DMSO): δ = 7.95 (s, 1H), 4.01 (s, 3H), 3.93 (s, 3H), 2.84 (s, 3H) ppm. **¹³C-NMR (125 MHz, d₆-DMSO):** δ = 160.6, 159.2, 117.5, 62.5, 39.6, 15.4 ppm. **HRMS (ESI, positive):** 144.04776 calculated for C₆H₁₀NOS⁺ [M]⁺, 144.04772 found.

Part B: Photocharacterisation in vitro

Spectrophotometry methods

Absorption spectra in cuvette (“UV-Vis”) were acquired on a Cary 60 UV-Vis spectrophotometer (1 cm pathlength). For photoisomerisation measurements, Hellma microcuvettes (108-002-10-40) taking 500 μL volume to top of optical window were used with the default test solution concentrations of 25 μM. Measurements were performed in PBS at pH~7.4 with 10% of DMSO. Photoisomerisations were performed at room temperature. Medium-power LEDs (H2A1-models spanning 360–490 nm from

Roithner Lasertechnik) were used to deliver high-intensity and relatively monochromatic light (FWHM ~25 nm) into the cuvette, for rapid PSS determinations that were also predictive of what would be obtained in LED-illuminated cell culture (Fig S1). Spectra of pure *E* and *Z* isomers were acquired from the inline Diode Array Detector during analytical separation on the HPLC (injection of 10 μ L, 5 \rightarrow 100% MeCN:H₂O over 20 min), after injecting DMSO stocks (0.5 – 2.5 mM) that had been irradiated with a 420 nm LED (~ 5 min) (Fig S2).

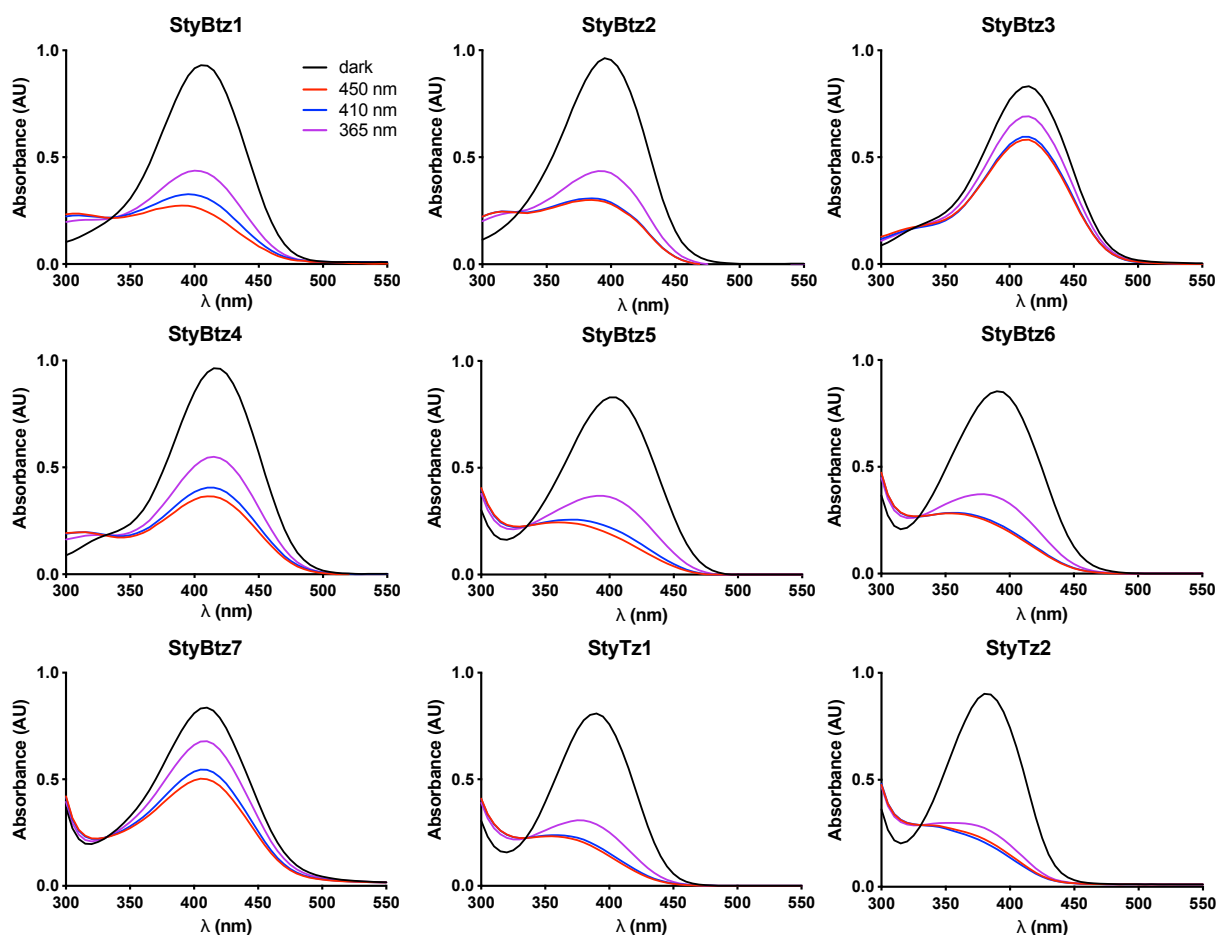


Fig S1 UV-Vis spectra at various photostationary states (ca. 25 μ M in PBS, pH ~7.4, 10% DMSO, room temperature, under closed air atmosphere)..

Para-hydroxy **StyBtz4**, that is inductively acidified by *N*-alkylation, was likely deprotonated to zwitterionic/quinoial species in water at/above pH=7, as indicated by the deeper red colour of its test solutions compared to those of other compounds.

Overall, StyBtz/StyTz photochemistry was similar to that previously described^[15,21].

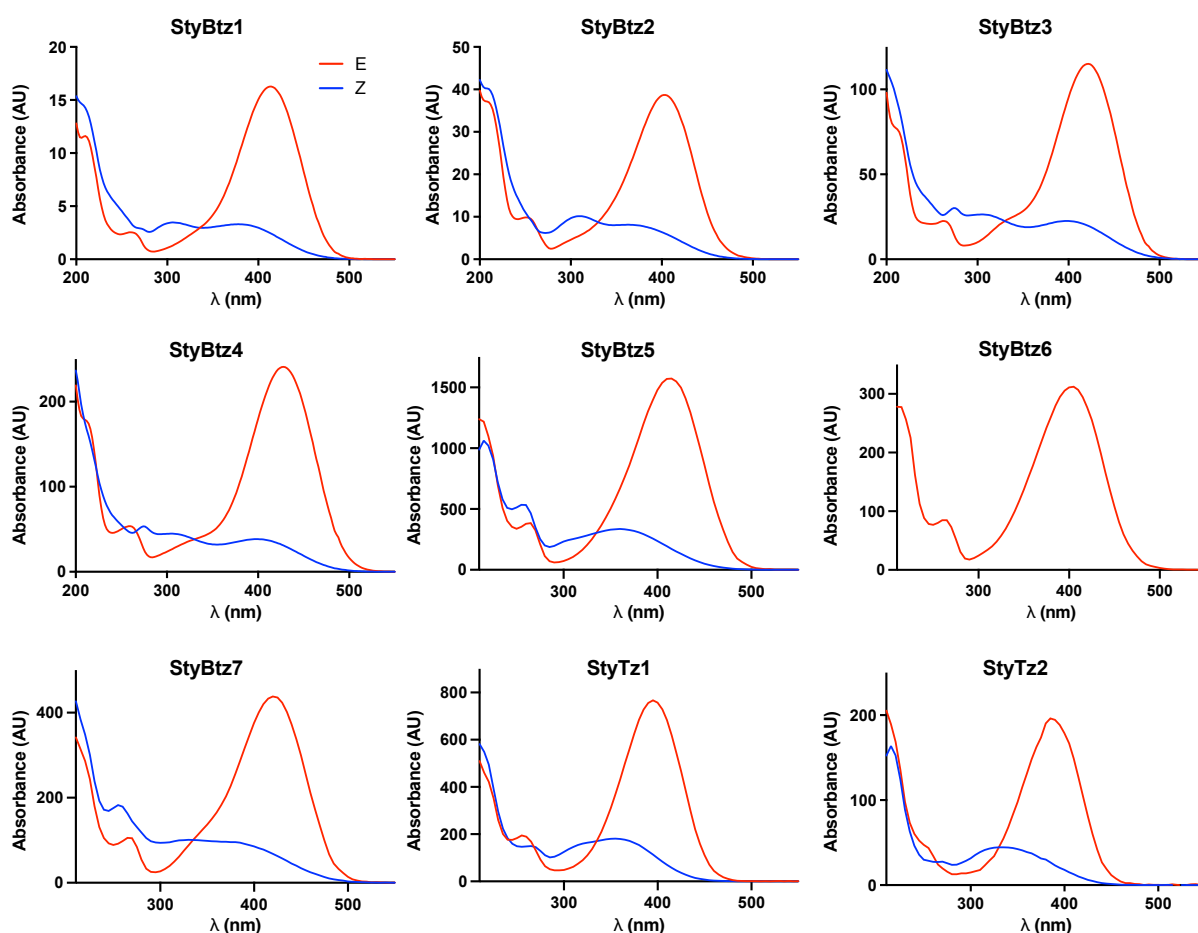


Fig S2 Isolated *E* and *Z*-spectra of **StyBtz** and **StyTz** obtained from inline DAD on HPLC (acidic media).

Spontaneous relaxation

Solutions of **StyBtz** and **StyTz** (25 μM in PBS + 10% DMSO) were prepared from DMSO stock solutions of **StyBtz** and **StyTz** kept in the dark at 60°C overnight. Spontaneous relaxation was measured by following the change of absorption at $\lambda(E)_{\text{max}}$ over time, while first establishing a “dark adapted” baseline for 4 min (until $t=0$ min), then irradiating with 450 nm for 1 min, then following relaxation thereafter (**Fig S3**).

Comparing the half-lives of **StyBtz1** with **StyBtz2** and **StyBtz5** with **StyBtz6** showed that 3,4,5-trimethoxy substitution gives faster $Z \rightarrow E$ spontaneous relaxation than 2,3,4-trimethoxy substitution. Comparing **StyBtz3** with **StyBtz4** shows that isovanillyl gives slower relaxation than vanillyl, likely because free rotation around the C-C single bond of the *para*-hydroxy **StyBtz4**'s quinoidal tautomer (see comment to **Fig S1**) increases its $Z \rightarrow E$ relaxation speed.

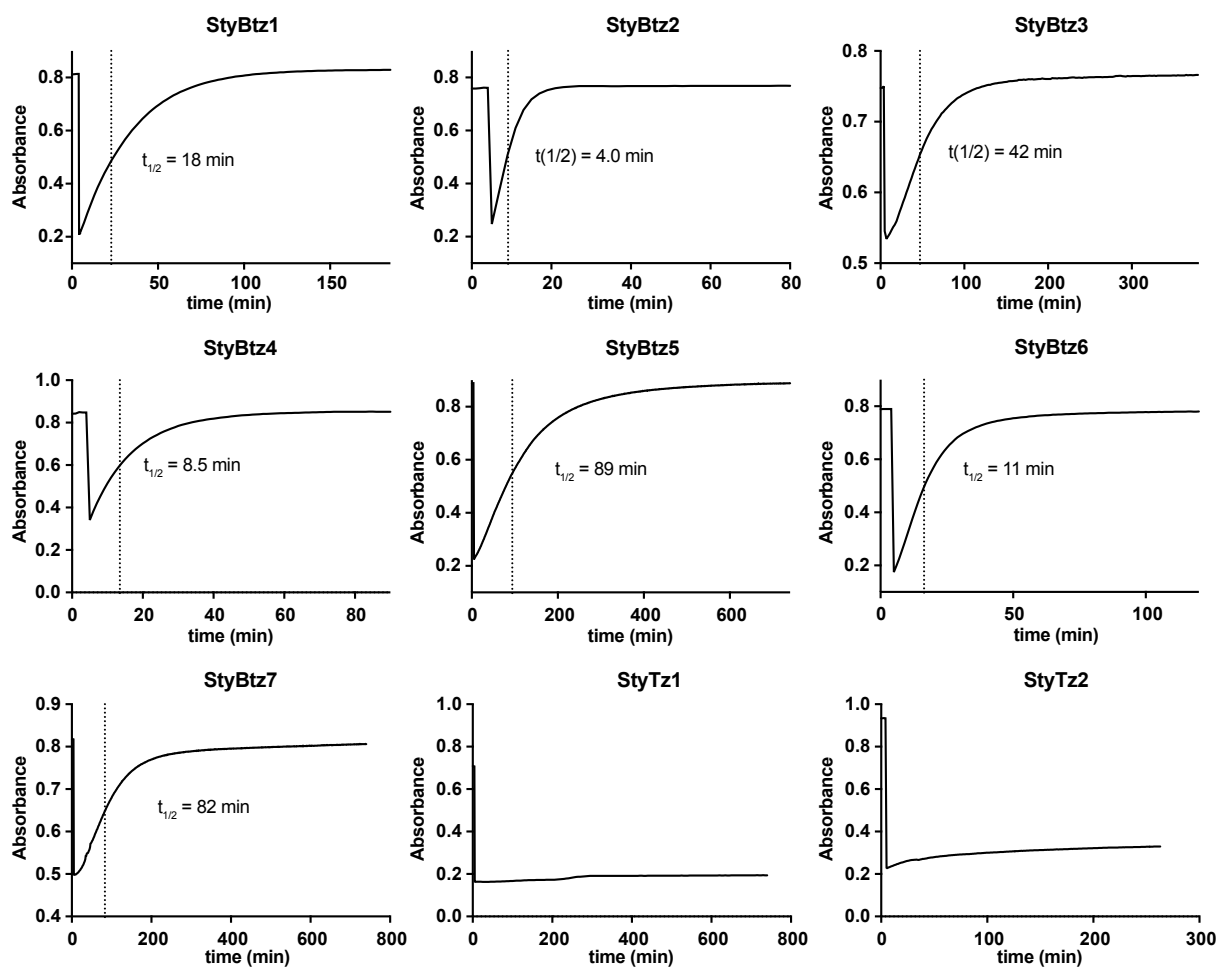


Fig S3 Spontaneous $Z \rightarrow E$ relaxation in the dark at room temperature (22°C) after illuminating dark adapted (all- E) samples of **StyBtz** and **StyTz** ($25 \mu\text{M}$, PBS pH ~ 7.4 + 10% DMSO) with 450 nm light for 1 min.

pH dependence of spontaneous relaxation rate

Solutions of **StyBtz1-3** in deionised water at pH = 7, and in deionised water adjusted to pH = 5 or 9, were prepared ($\sim 25 \mu\text{M}$). Spontaneous relaxation was measured by following the change of absorption at $\lambda(E)_{\text{max}}$ over time, while first establishing a “dark adapted” baseline for 4 min (until $t=0$ min), then irradiating with 450 nm for 1 min, then following relaxation thereafter (**Fig S4**).

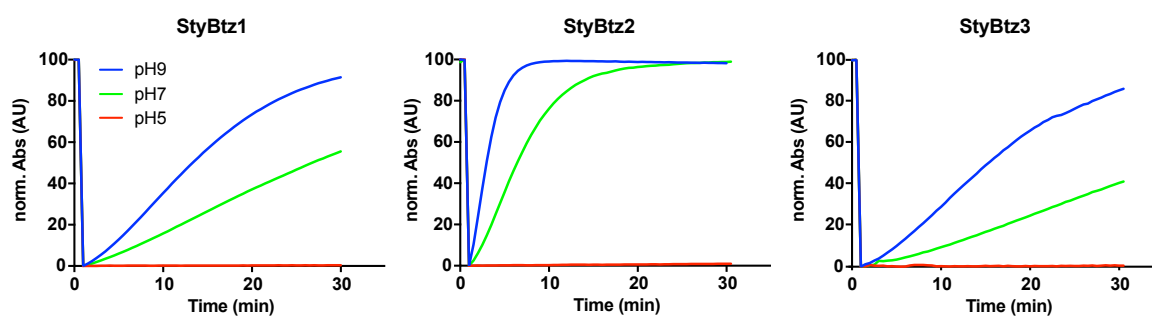


Fig S4 pH dependencies of the relaxation rates (room temperature). Absorbance readings have been translated vertically and scaled so that the absorbance value in the dark adapted state is 100, and the absorbance value at PSS 450 nm is 0, allowing easier comparison of relaxation rates.

Spontaneous $Z \rightarrow E$ relaxation of **StyBtz** was strongly pH-dependent; at pH 9 it was twice as fast as at pH 7, and in mild acid (pH 5), spontaneous $Z \rightarrow E$ isomerization was completely stopped.

Solvent dependence of spontaneous relaxation

Solutions of **StyBtz1-3** in DMSO, MeCN, EtOH and EtOAc were prepared (final concentration $\sim 25 \mu\text{M}$). Spontaneous relaxation was measured by following the change of absorption at $\lambda(E)_{\text{max}}$ over time, while first establishing a “dark adapted” baseline for 4 min (until $t=0$ min), then irradiating with 450 nm for 1 min, then following relaxation thereafter (**Fig S5**).

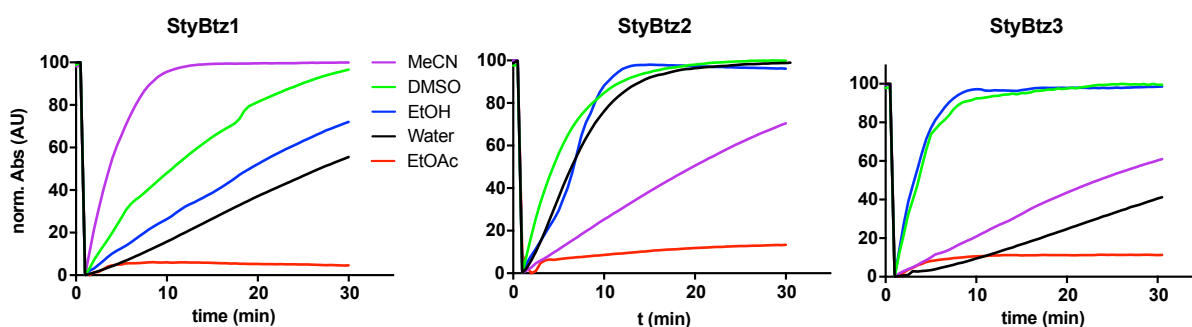


Fig S5 Solvent dependencies of the relaxation rates (room temperature). Absorbance readings have been translated vertically and scaled so that the absorbance value in the dark adapted state is 100, and the absorbance value at PSS 450 nm is 0, allowing easier comparison of relaxation rates. Deionised water used.

Fluorescence measurement

Solutions of **StyBtz1-4** ($25 \mu\text{M}$ in PBS + 0.1% DMSO + 0.1% FA) were prepared in Hellma microcuvettes (101-10-40). Fluorescence ex/em spectra were measured on a Varian Cary Eclipse fluorescence spectrometer (**Fig S6**).

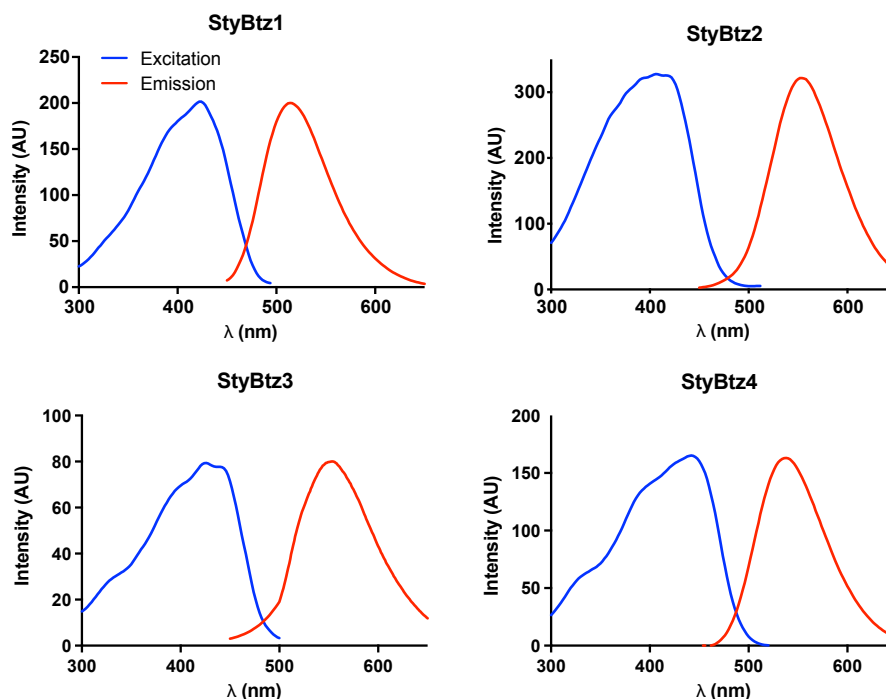


Fig S6 Fluorescence excitation and emission spectra of **StyBtz1-4** ($25 \mu\text{M}$ in PBS + 0.1% DMSO + 0.1% FA).

PSS measurements; comparison to calculated $\phi(\lambda)$; estimated $E(\lambda)$

Estimation of the E/Z ratio at any wavelength's photostationary state (PSS) was done by comparing experimentally measured UV-spectra from different PSS equilibria, with calculated PSS spectra as previously described^[2] (Fig S7).

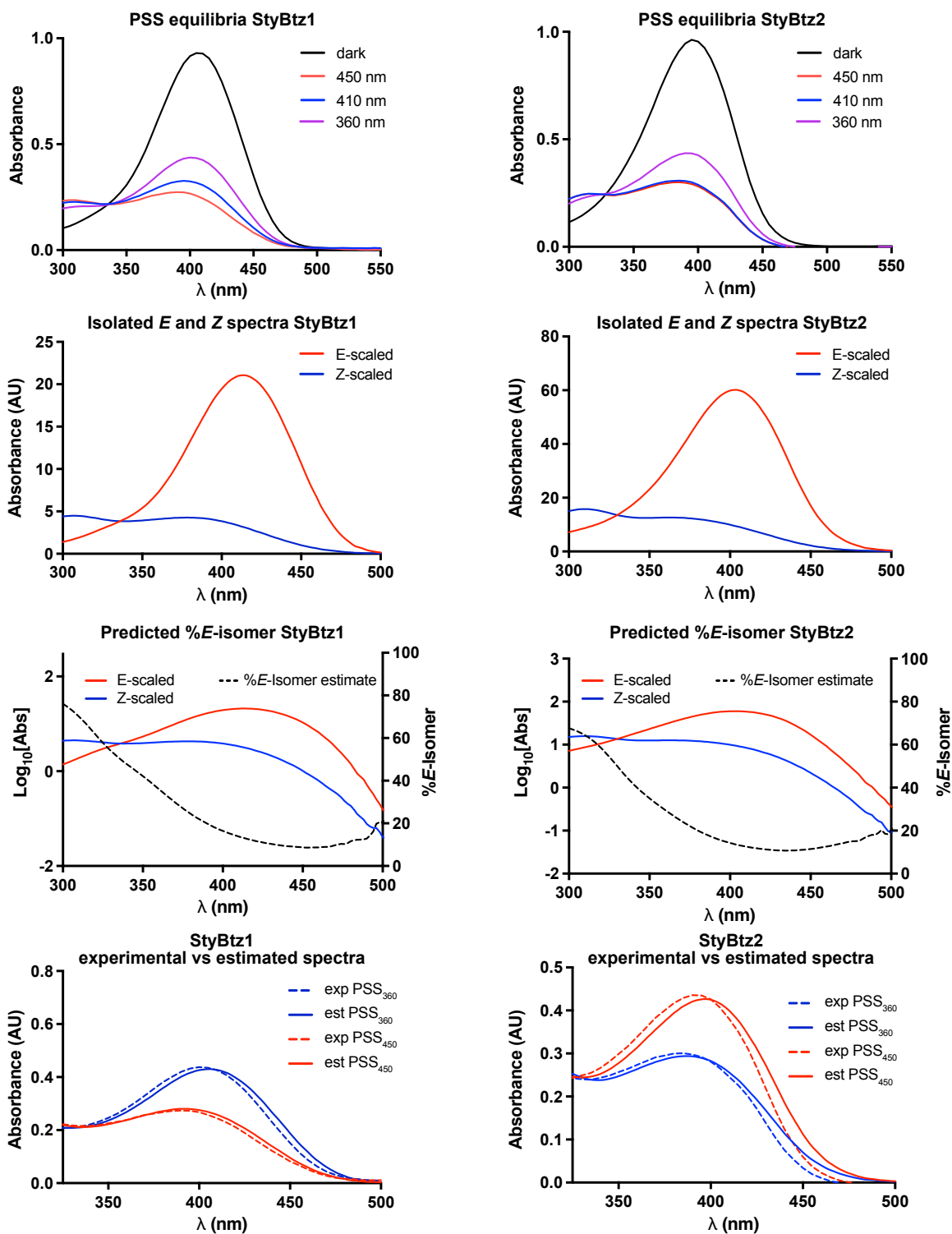


Fig S7 PSS measurements and their comparison to simulated PSS(λ) returned from the PSS estimate analysis.

Photosensitization assay

To assess the photosensitization properties of **StyBtz2** the change of absorbance at 410 nm was observed from photobleaching of 1,3-diphenylbenzofuran (DPBF). First, 5 mM DPBF in isopropanol, 1 mM StyBtz2 in DMSO and 0.5 mM methylene blue stock solutions were prepared. The measurements were carried out (**Fig S8a-c**): **(a) DPBF + light** Background measured on pure isopropanol. 2.5 μL of DPBF (5 mM) added to 248 μL of isopropanol in a 250 μL black quartz cuvette (final volume 250 μL , final concentration DPBF 50 μM). Start measurement (scan every 6 seconds) and cuvette illumination with 450 nm light. **(b) DPBF + light + StyBtz2** Prepare blank for baseline measurement: 2.5 μL of **StyBtz2** (1 mM in DMSO) add to 245 μL of isopropanol, illuminate with 450 nm light until PSS is reached and record background (this is to take out the $\pi \rightarrow \pi^*$ band of **StyBtz2** which overlaps with the absorption band of DPBF). Then, add 2.5 μL of DPBF (final concentration DPBF 50 μM , StyBtz2 10 μM) and start measurement immediately while illuminating with 450 nm light. **(c) DPBF + light + MB** background of pure isopropanol recorded. 2.5 μL of 0.5 mM methylene blue (MB), then 2.5 μL of DPBF added to 245 μL of isopropanol. Scan spectra while illuminating with 660 nm light (final concentration DPBF 50 μM , MB 5 μM). Absorbance at 410 nm was plotted against time in minutes (**Fig 3f**) to compare the rate of DPBF photobleaching between measurements a-c after normalization (1.0 = Abs_{410 nm} at t = 0 min, 0.0 = no absorbance at 410 nm).

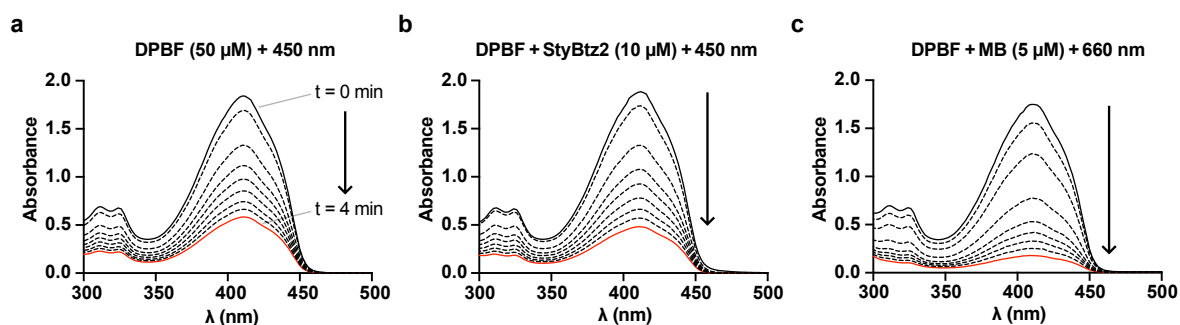


Fig S8 DPBF (50 μM) photobleaching over time (4 min) under **(a)** 450 nm light **(b)** 450 nm light and **StyBtz2** (10 μM) **(c)** 660 nm light and MB (5 μM).

Part C: Biological and Biochemical Data

Cell culture and illuminations in cell culture

Cell culture was performed under standard conditions (37°C, 5% CO₂), maintaining HeLa cells in Dulbecco's modified Eagle's medium (DMEM; PAN-Biotech: P04-035550) supplemented with 10% fetal calf serum (FCS), 100 U/mL penicillin and 100 U/mL streptomycin, as described in detail previously.^[22] As described previously^[1] and as implemented across a range of long-term cell culture studies^[2,22,23], compounds were applied to cells in the all-*E* state, then treated cells were either incubated under "dark" conditions (incubation in lightproof boxes in the incubator) or "lit" conditions {wellplates incubated sitting on top of 24-LED arrays of our home-made "Disco" system (ca. 1.5 cm away from the LED emitter chips, that are packaged as 5 mm ball lens LEDs operated at 20 mA / ca. 4V, with central wavelength 450 nm (FWHM ca. 25 nm) unless stated otherwise) that is controlled by Arduino to deliver pulsed illuminations reaching ca. 3 mW / cm² optical output intensity at the cells^[1]: i.e. a comparatively low intensity, and with low duty cycle of typically 75 ms pulses applied every 15 s unless stated otherwise}. We have found this default timing pattern for this low intensity and duty cycle to be tolerated in the visible/nUV spectrum by all cell lines we have worked with; additionally, our studies explicitly confirmed it is tolerated *in the presence of* various photoswitch scaffolds without phototoxic effects. The "75 ms per 15 s" frequency is intended to prevent StyBtz with seconds-to-minutes relaxation timescales from reverting substantially to the thermodynamic ground state between pulses, so that the long-term assay evaluation *should* reflect isomer-dependent bioactivity in a way that is predictive of acute isomer-dependent pharmacology in short-term assays (the targeted use-scenario of the compounds.)

Resazurin antiproliferation assay

HeLa cells were seeded in 96-well plates at 5,000 cells/well and left to adhere for 24 h before treating with test compounds. *E*-StyBTz/StyTz were added for 48 h (final well volume 100 µL, 1% DMSO; three technical replicates); the "cosolvent control" ("ctrl") indicates treatment with DMSO only. Cells were then treated with resazurin 150 mg/mL for 3 h. Fluorescence was measured at 590 nm (excitation 544 nm) using a FLUOstar Omega microplate reader (BMG Labtech). Absorbance data was averaged over the technical replicates, then normalized to viable cell count from the cosolvent control cells (%control) as 100%, where 0% viability was assumed to correspond to fluorescence signal in PBS only with no cells. One experiment out of three independent experiments is shown. Data were plotted against the log of compound concentration (e.g. log₁₀([StyBtz]) (M)) showing mean and SD (**Fig S9**).

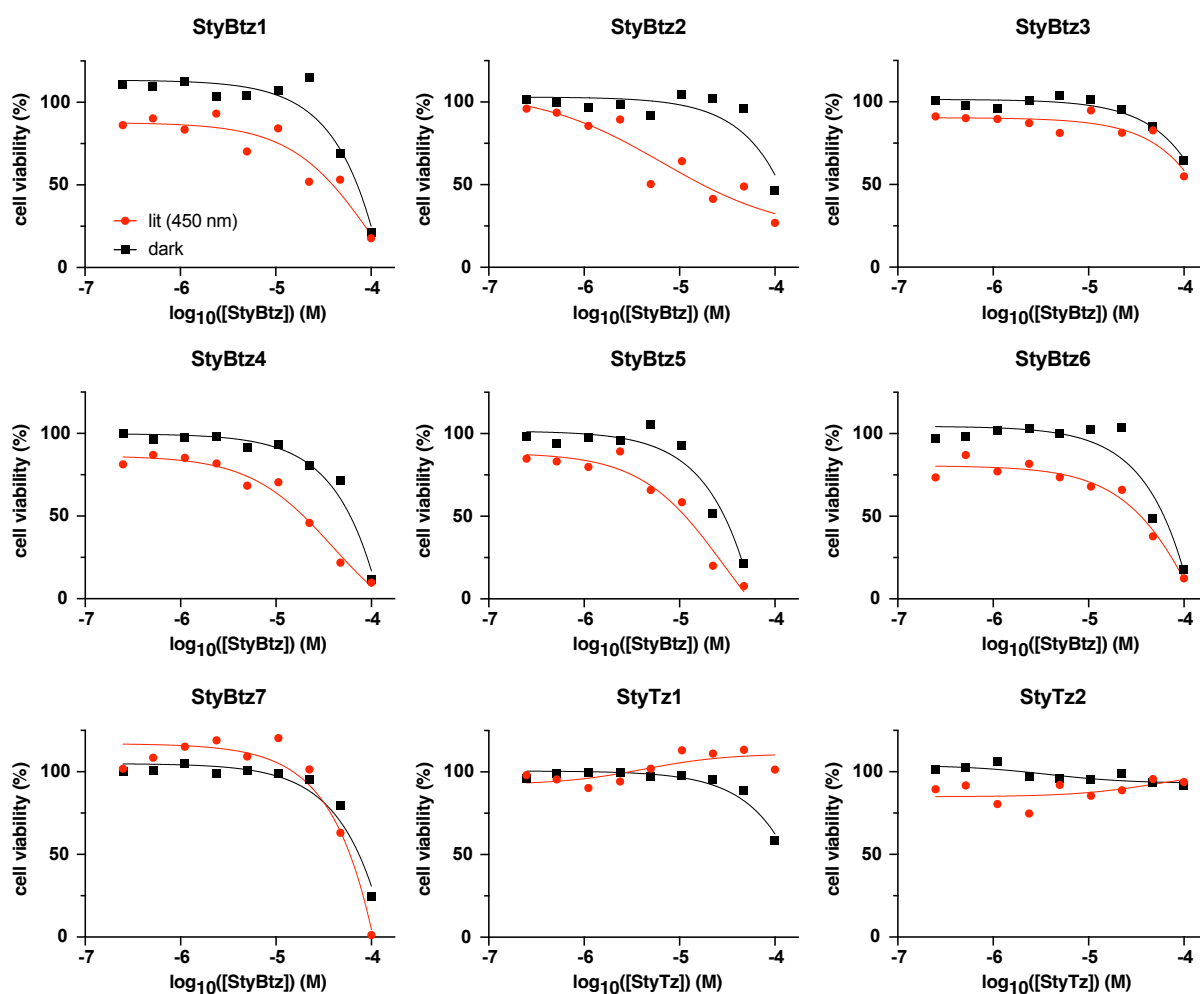


Fig S9 Antiproliferation assay of StyBtz and StyTz in HeLa cells. 40 h incubation; all-*E* dark conditions versus lit conditions with predominantly *Z*-isomer using low-power pulsed LED illuminations (75 ms per 15 s, <1 mW/cm²); HeLa cells, one representative experiment out of three independent experiments shown.

Immunofluorescence

HeLa cells were seeded on glass coverslips in 24-well plates (50,000 cells/well) and treated with **StyBtz2** the next day under “dark” or “lit” conditions for 24 h. Cells were fixed and permeabilised in ice-cold methanol for 5 min, then washed and kept in PBS at 4°C until staining. Samples were equilibrated to room temperature and blocked with PBS + 1% BSA for 30 min. Cells were treated with primary antibody (1:200 rabbit alpha-tubulin; Abcam ab18251) in PBS/1% BSA/0.1% Triton X-100 overnight and with secondary antibody (1:500 goat-antirabbit Alexa Fluor 488; Abcam ab150077) in PBS/1% BSA/0.1% Triton X-100 for 1 h. Coverslips were mounted onto glass slides using Roti-Mount FluorCare DAPI (Roth) and imaged with a Zeiss LSM710 confocal microscope (CALM platform, LMU). Images were processed using the free Fiji software¹¹ and Affinity Designer (Serif) for clarification. Postprocessing was only performed to improve visibility (**Fig S10**).

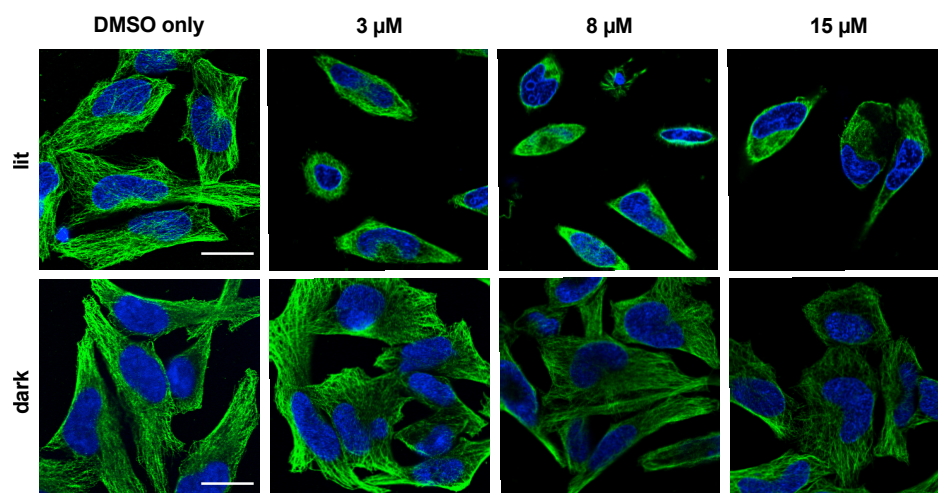


Fig S10 Immunofluorescence imaging of cells treated with **StyBtz2** shows disruption of MT architecture under 450 nm pulsing (“lit”) but no disorganization in the dark. DMSO only cosolvent control shows no light-dependent confounding effects (HeLa cells, 20 h incubation; α -tubulin in green, DNA stained with DAPI in blue). Scale bars, 20 μ m.

Cell cycle analysis

E-StyBtz1-4 (15 μ M) were added to HeLa cells in 24-well plates (50,000 cells/well; three technical replicates, three biological replicates) and incubated under “dark” or “lit” conditions for 24 h. Cells were collected, permeabilised and stained with 2 μ g/mL propidium iodide (PI) in HFS buffer (PBS, 0.1% Triton X-100, 0.1% sodium citrate) at 4°C for 30 min then analysed by flow cytometry using a FACS Canto II flow cytometer (Becton Dickinson) run by BD FACS Diva software (**Fig S11**).

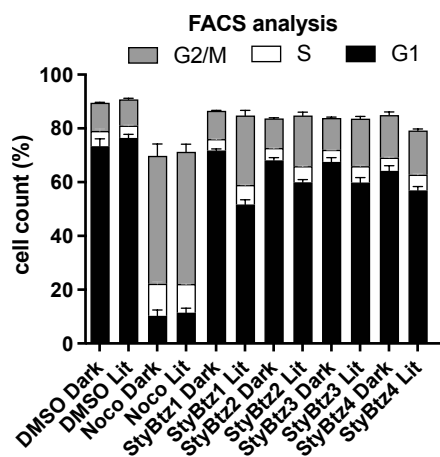


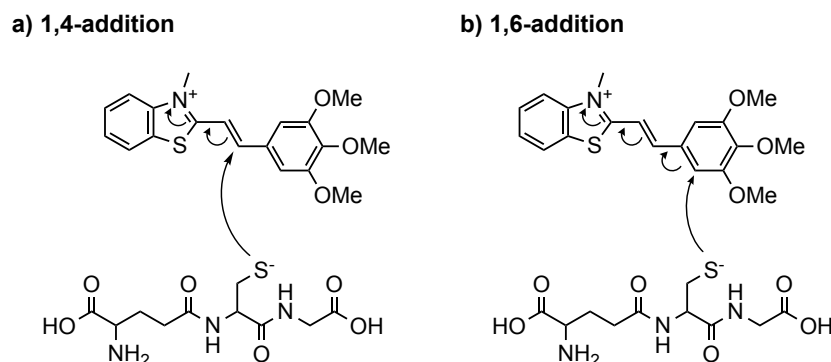
Fig S11 Cell cycle partitioning shows no cell cycle effects of **StyBtz1-4** (15 μ M) in HeLa cells comparable to the DMSO only cosolvent controls. Typical antimetabolic agents such as nocodazole usually exhibit G2/M arrest.

Stability to glutathione

5 μ L of 2.5 mM solution of **StyBtz2** in DMSO was added to 495 μ L of 10 mM glutathione (GSH) in PBS pH ~ 7.4 in a UV-Vis cuvette (final concentration 25 μ M, PBS + 1% DMSO), similar to published procedures^[24]. The absorbance was measured as a function of time in a Varian Cary 60 spectrophotometer at 22°C showing that **StyBtz2** was highly sensitive to glutathione ($t_{1/2} < 2$ min), with complete depletion of the photoswitch within 10-15 min (**Fig 3e**) probably by 1,4-conjugate addition of GSH (Scheme S1). Although 1,6-conjugate addition, or *N*-demethylation, are also possible, we do not

consider them likely: *N*-demethylation would result in liberation of the highly bioactive tubulin-binding SBTs, which is inconsistent with our cellular data; and 1,6-addition would disrupt aromaticity; whereas 1,4-addition is preceded by similar reactions of large nucleophiles such as phosphines^[12].

Scheme S1: Likely 1,4-conjugate addition of glutathione to **StyBtz2**, and alternative possibility of 1,6-addition.



Tubulin polymerisation assay

Purified tubulin from calf brain was obtained from CSIC (Spain). The polymerisation reaction was performed at 2 mg/mL tubulin, in BRB80 polymerisation buffer (80 mM piperazine-*N,N'*-bis(2-ethanesulfonic acid) (PIPES), 0.5 mM EGTA, 2 mM MgCl₂, pH = 6.9), in a cuvette (100 μ L, 1 cm path length) in a Varian CaryScan 60 with Peltier cell temperature control unit maintained at 37°C, with final concentrations of 3% DMSO and 5% glycerol by volume. Tubulin was incubated for 5 min at 37°C optionally with reference tubulin inhibitors nocodazole ("noco"; MT destabilizer; 2 μ M) or docetaxel (MT stabilizer; 1 μ M), or else with **StyBtz2** (20 μ M); then, GTP (final concentration 1 mM) was added and the solution mixed by pipetting up and down for 5 s to initiate polymerisation, then absorbance at 340 nm was zeroed; absorbance was then measured every 15 s to monitor. Nocodazole/docetaxel were not illuminated in the experiment; **StyBtz2** was either kept in the dark or was continuously illuminated at 450 nm for lit conditions; using a monochromator-liquid light guide setup (ca. 3 mW/cm²; FWHM 10 nm) (**Fig 3d**). We prefer nocodazole as a reference destabiliser over CA4 or colchicine, since with UV illumination, CA4 can partially isomerise to *trans* but also undergoes 6 π -electrocyclisation that is irreversibly trapped by oxidation; and colchicine is irreversibly electrocyclicised to biologically inactive lumicolchicine, whereas nocodazole does not suffer these problems.

Live cell imaging

HeLa cells (12,000 cells/well) were seeded on 8-well ibiTreat m slides (ibidi) 24 h prior to transfection with fluorescently-labeled end binding protein. Cells were transiently transfected with EB3-GFP plasmids using jetPRIME (Polyplus) reagents according to the manufacturers' instructions. Cells were imaged 24 h later, under 37°C and 5% CO₂ atmosphere. HeLa cells were imaged using an UltraVIEW Vox spinning disc confocal microscope (PerkinElmer) equipped with an EMCCD camera (Hamamatsu, Japan) and operated with Volocity software. The microscope was controlled by Nikon NIS Elements software (v.5.02.00). **StyBtz2** was added cautiously after focussing on cells on the microscope stage, and the compound was incubated for 5-10 min before imaging; this avoided exposure of the StyBtz to any white focusing light, preventing unwanted isomerisation prior to imaging.

Cells were imaged with alternating pulses of 488 nm (GFP; 23% laser power, 400 ms exposure time) and 405 nm (StyBtz; 10% laser power, 200 ms) (**Fig 4a** and **Movie S1**). For mitochondria imaging, cells were treated with Mitotracker Red (0.5 μ M) that was imaged at 561 nm (20% laser power, 400 ms) (**Fig 4b** and **Movie S2**).

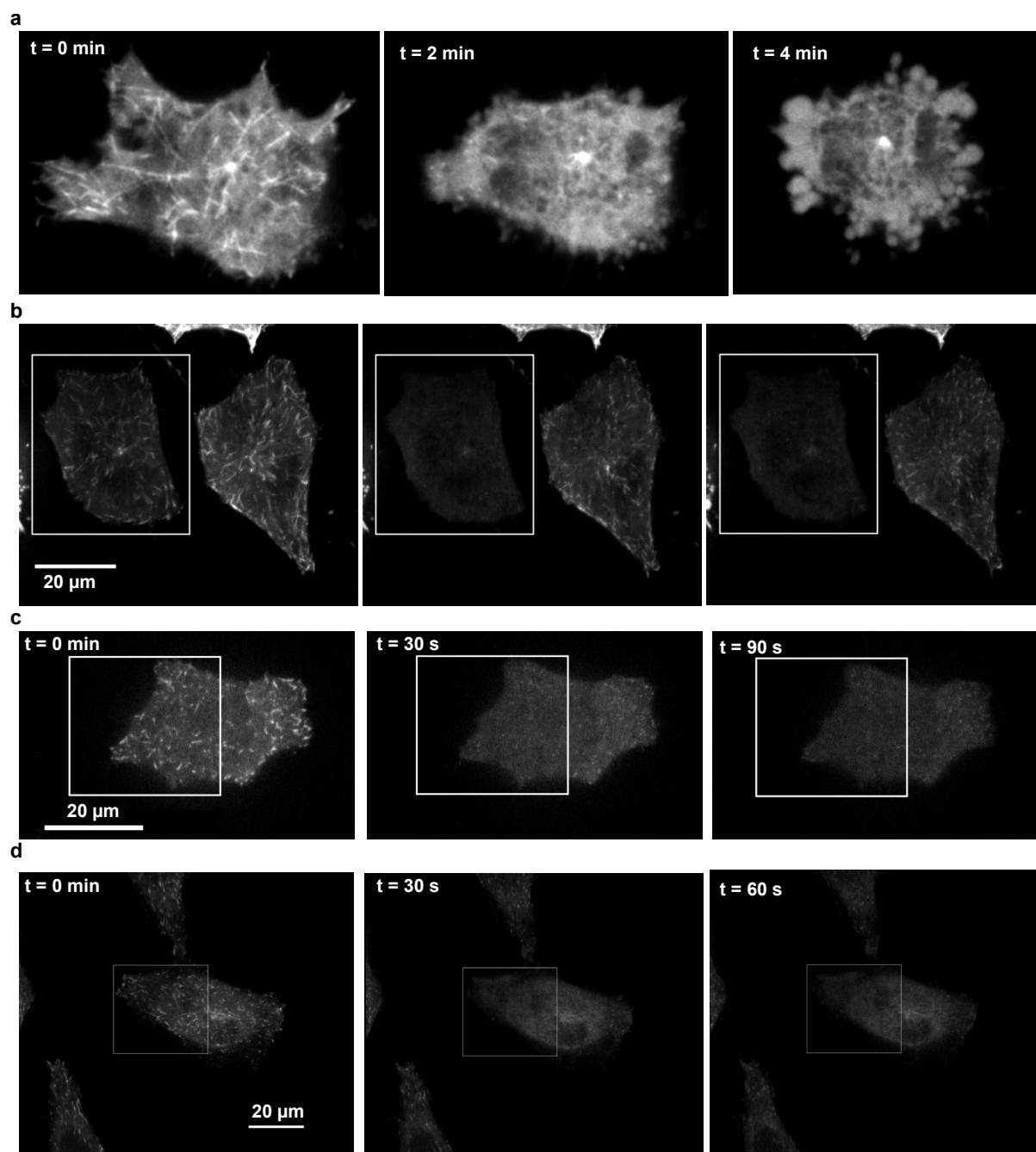


Figure S12. (a) induction of blebbing and detachment during minutes of photoswitching (**StyBtz2**, imaged as in **Fig 4**). t = 0 intact, then increasingly blebbed. (b) cell-targeted disruption by cell-localised ROI illumination (**StyBtz2**, 10 μ M, imaged at 488 nm, ROI illumination at 440 nm as indicated). (c-d) subcellularly-targeted disruption by subcellular ROI illuminations (at 440 or 405 nm as indicated).

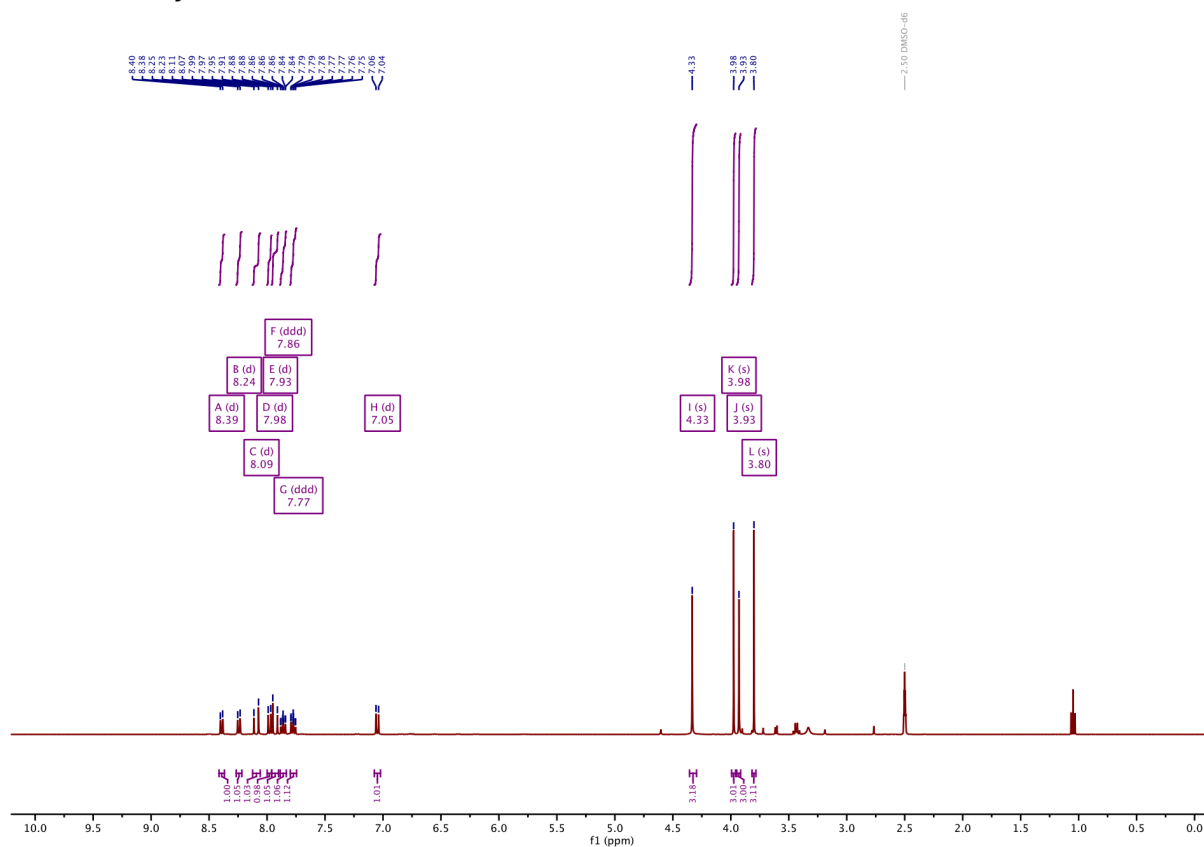
Part D: Crystallographic Data

Table S1 Crystallographic data **StyBtz2**

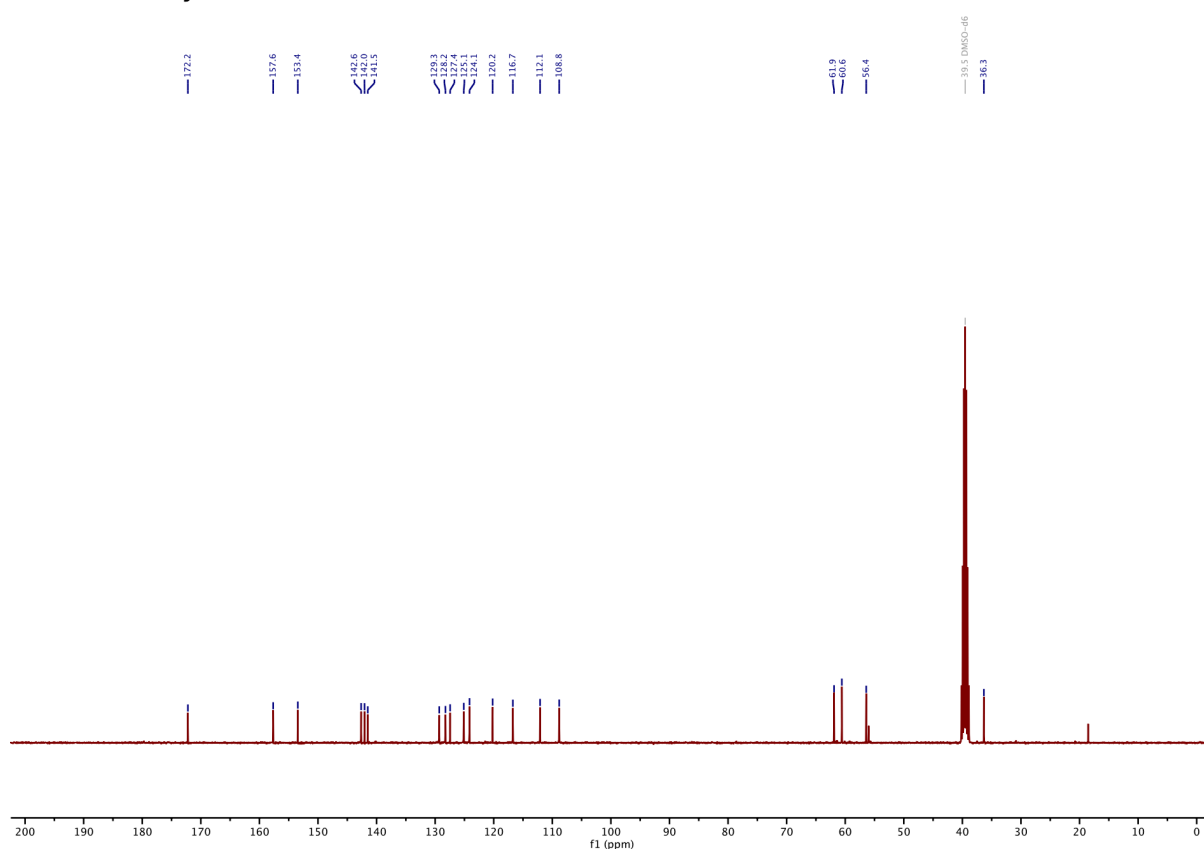
	StyBtz2 iodide
net formula	C ₁₉ H ₂₂ INO ₄ S
<i>M_r</i> /g mol ⁻¹	487.33
crystal size/mm	0.070 × 0.050 × 0.030
<i>T</i> /K	103.(2)
radiation	MoKα
diffractometer	'Bruker D8 Venture TXS'
crystal system	triclinic
space group	'P -1'
<i>a</i> /Å	9.9425(3)
<i>b</i> /Å	10.2918(3)
<i>c</i> /Å	10.7151(3)
α/°	62.2190(10)
β/°	83.8720(10)
γ/°	86.7380(10)
<i>V</i> /Å ³	964.48(5)
<i>Z</i>	2
calc. density/g cm ⁻³	1.678
μ/mm ⁻¹	1.792
absorption correction	Multi-Scan
transmission factor range	0.87–0.95
refls. measured	8869
<i>R</i> _{int}	0.0253
mean σ(<i>I</i>)/ <i>I</i>	0.0355
θ range	3.212–25.349
observed refls.	3243
<i>x</i> , <i>y</i> (weighting scheme)	0.0241, 0.4755
hydrogen refinement	H(C) constr, H(O) refall
refls in refinement	3510
parameters	247
restraints	0
<i>R</i> (<i>F</i> _{obs})	0.0221
<i>R</i> _w (<i>F</i> ²)	0.0566
<i>S</i>	1.073
shift/error _{max}	0.001
max electron density/e Å ⁻³	0.454
min electron density/e Å ⁻³	-0.403
CCDC deposition number	2164188

Part E: NMR Spectra

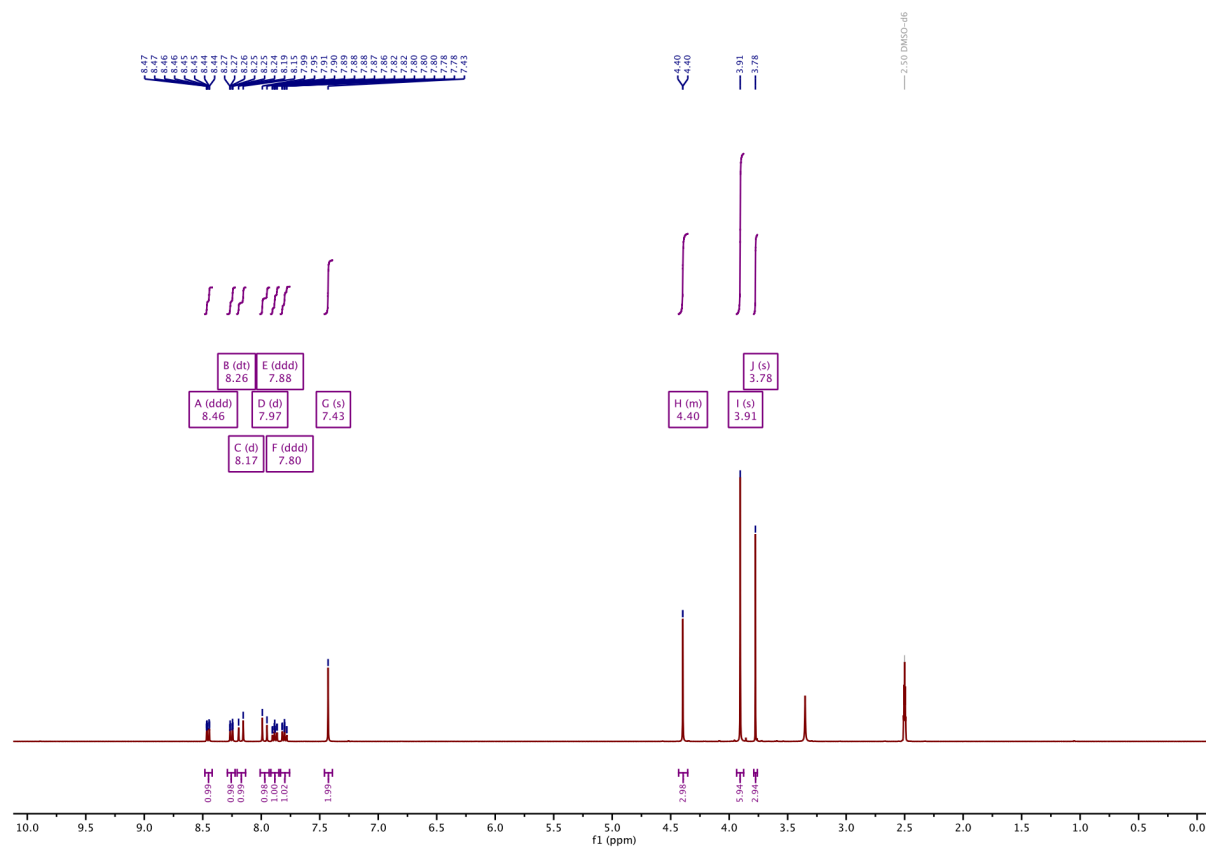
¹H-NMR of StyBtz1



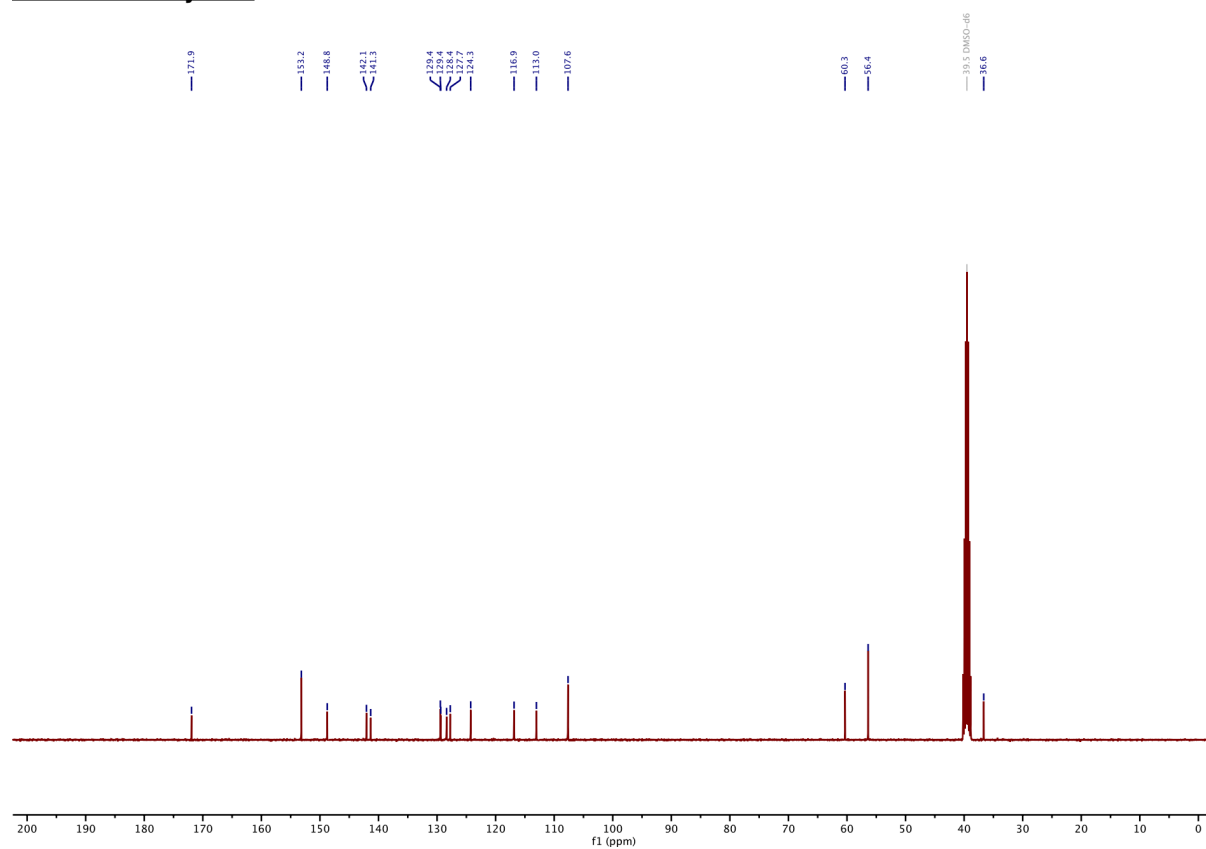
¹³C-NMR of StyBtz1



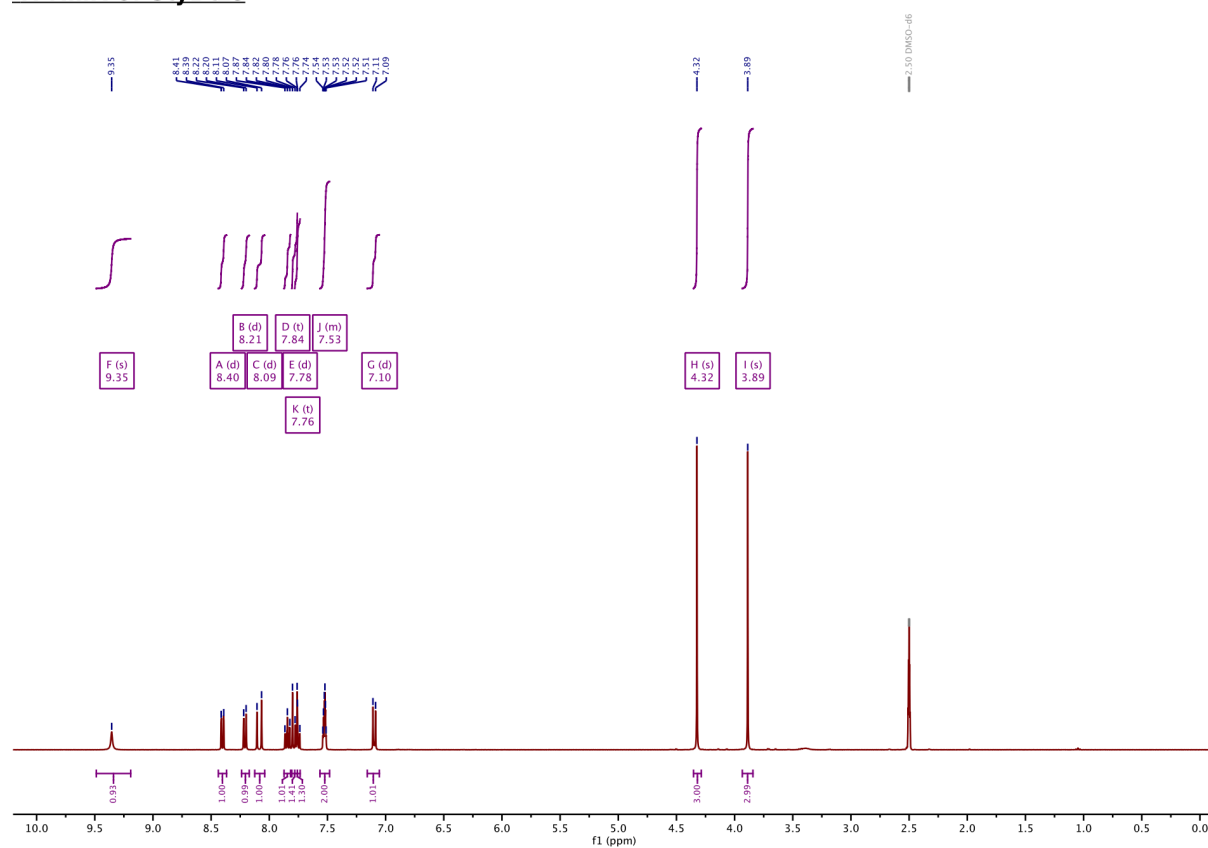
¹H-NMR of StyBtz2



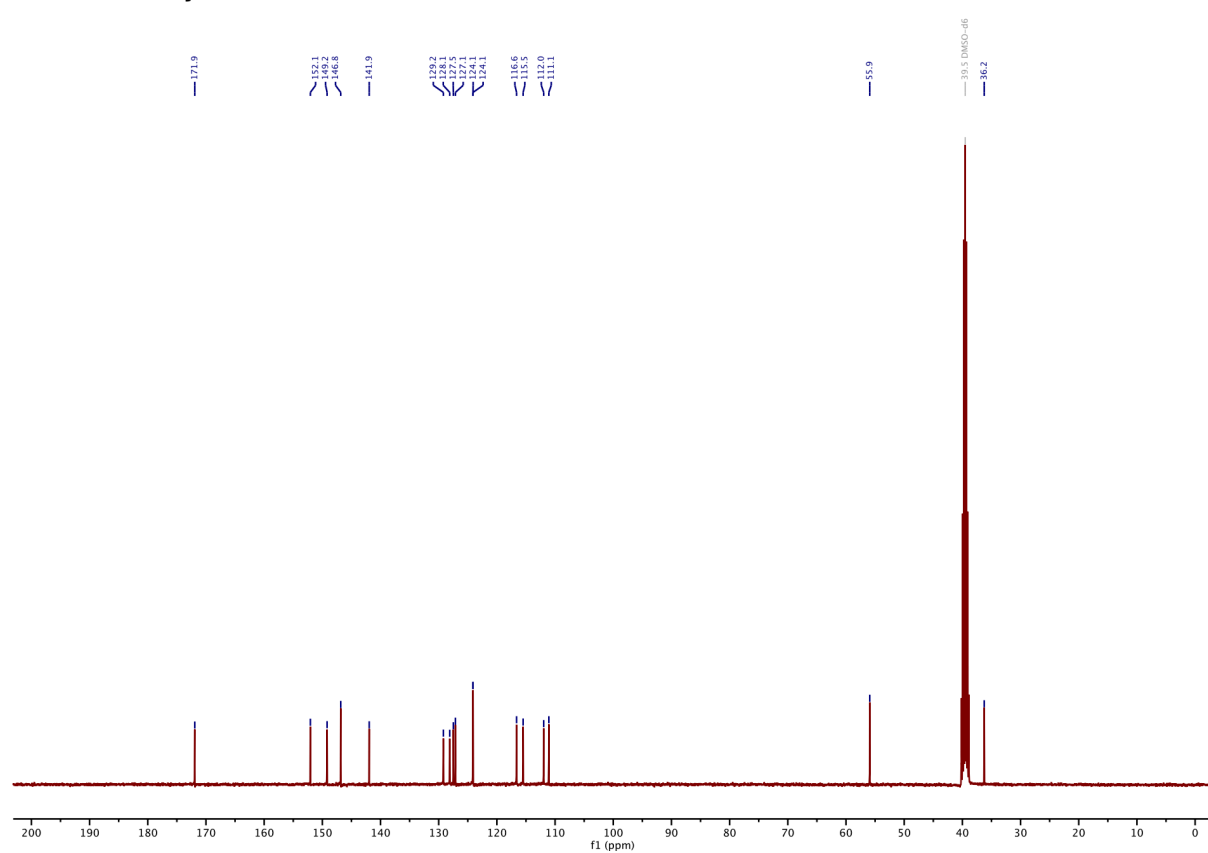
¹³C-NMR of StyBtz2



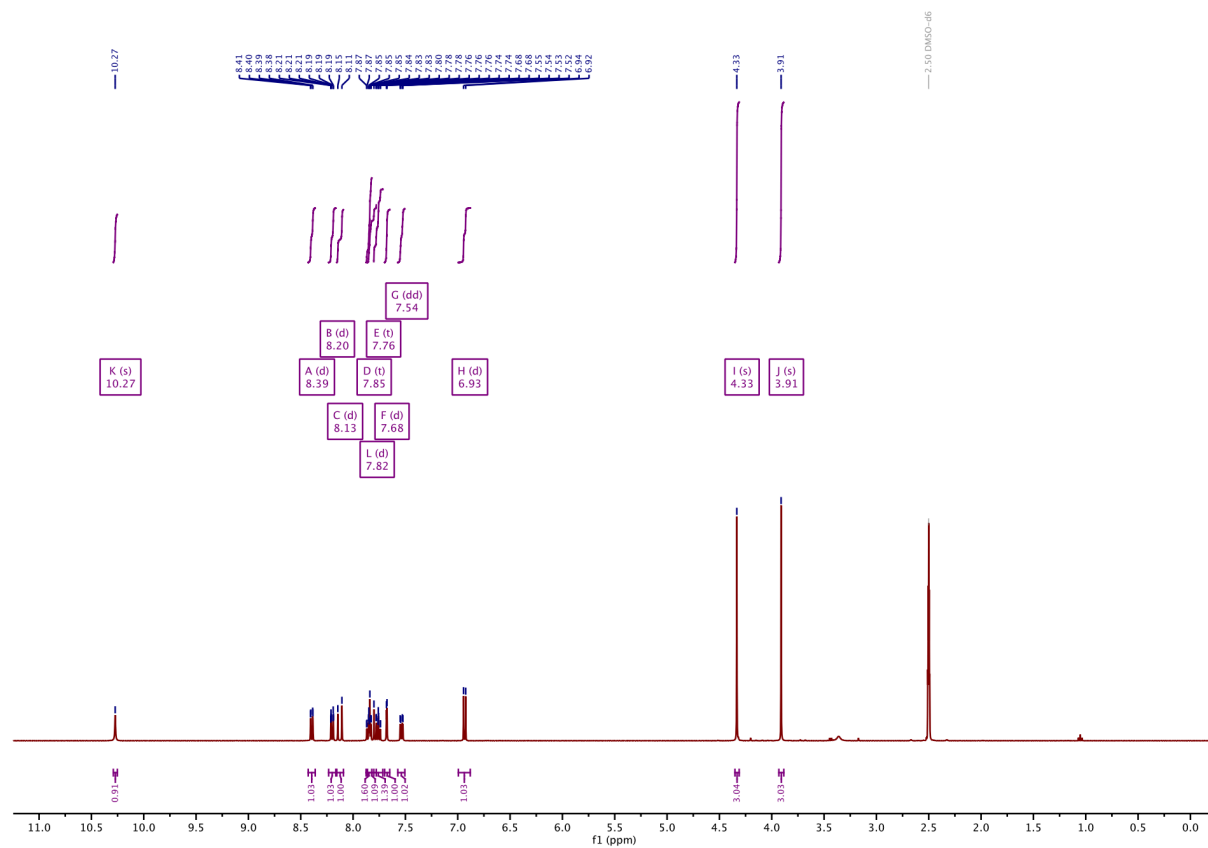
¹H-NMR of StyBtz3



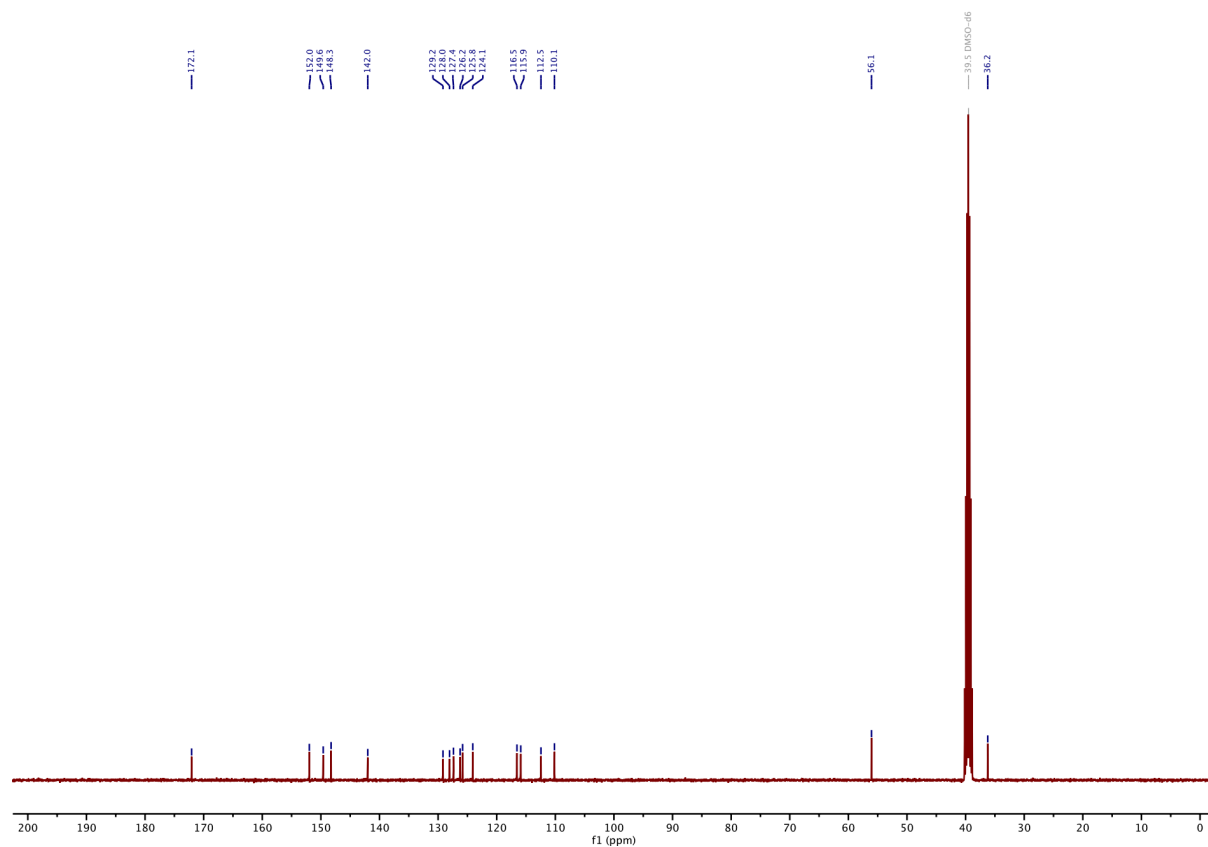
¹³C-NMR of StyBtz3



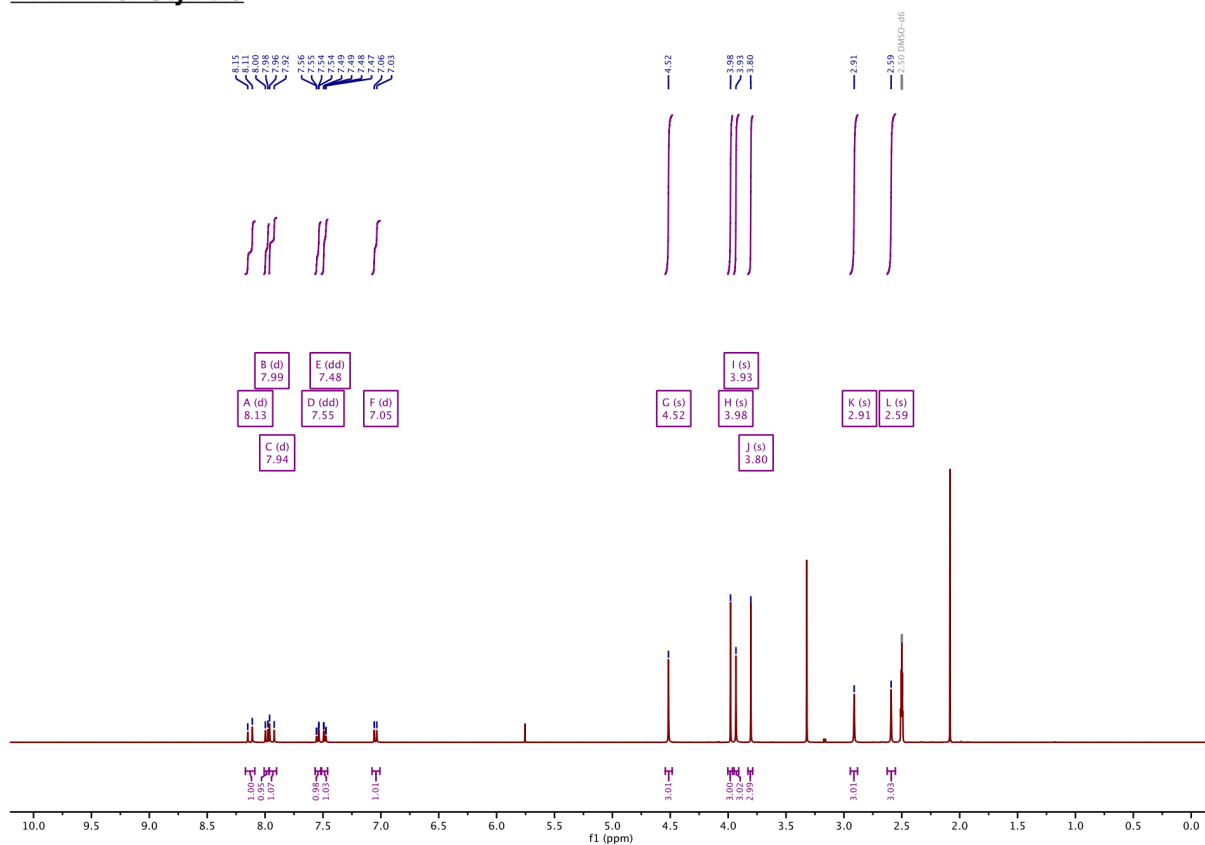
¹H-NMR of StyBtz4



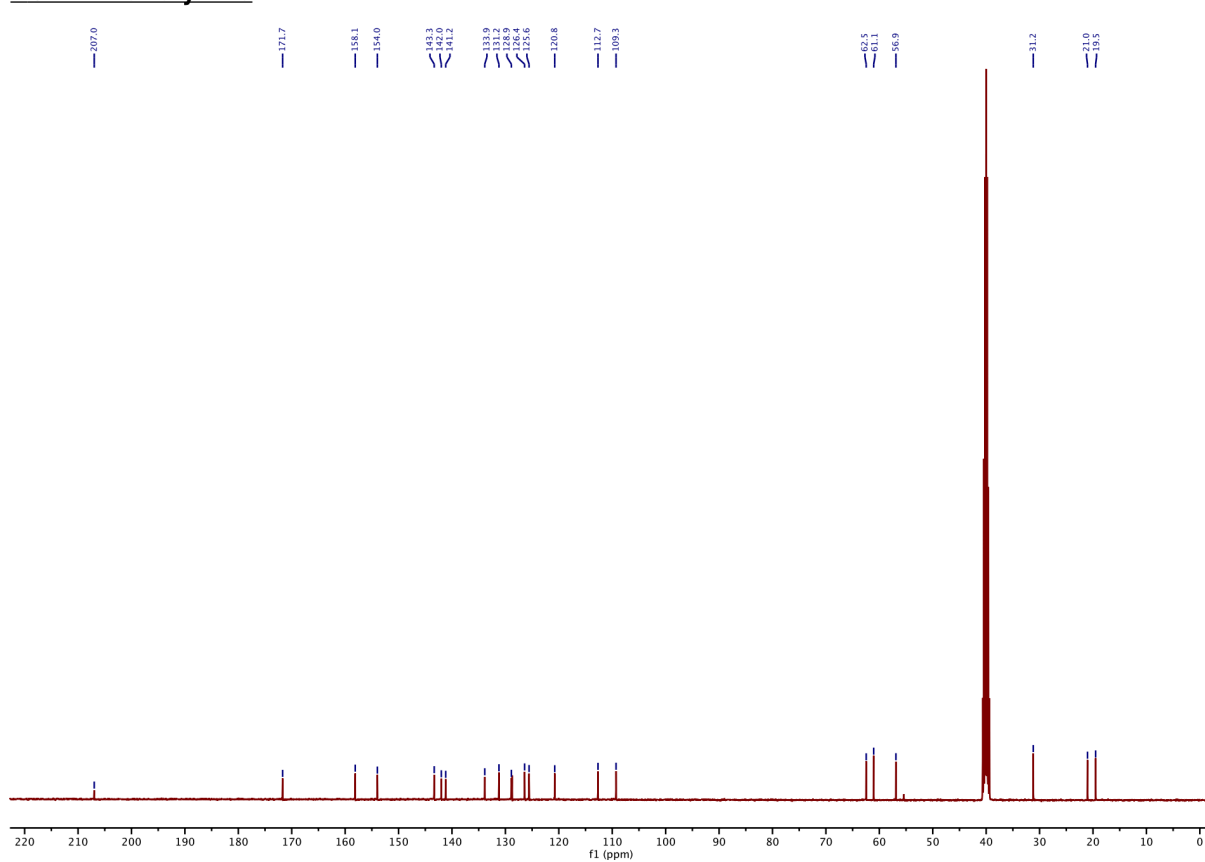
¹³C-NMR of StyBtz4



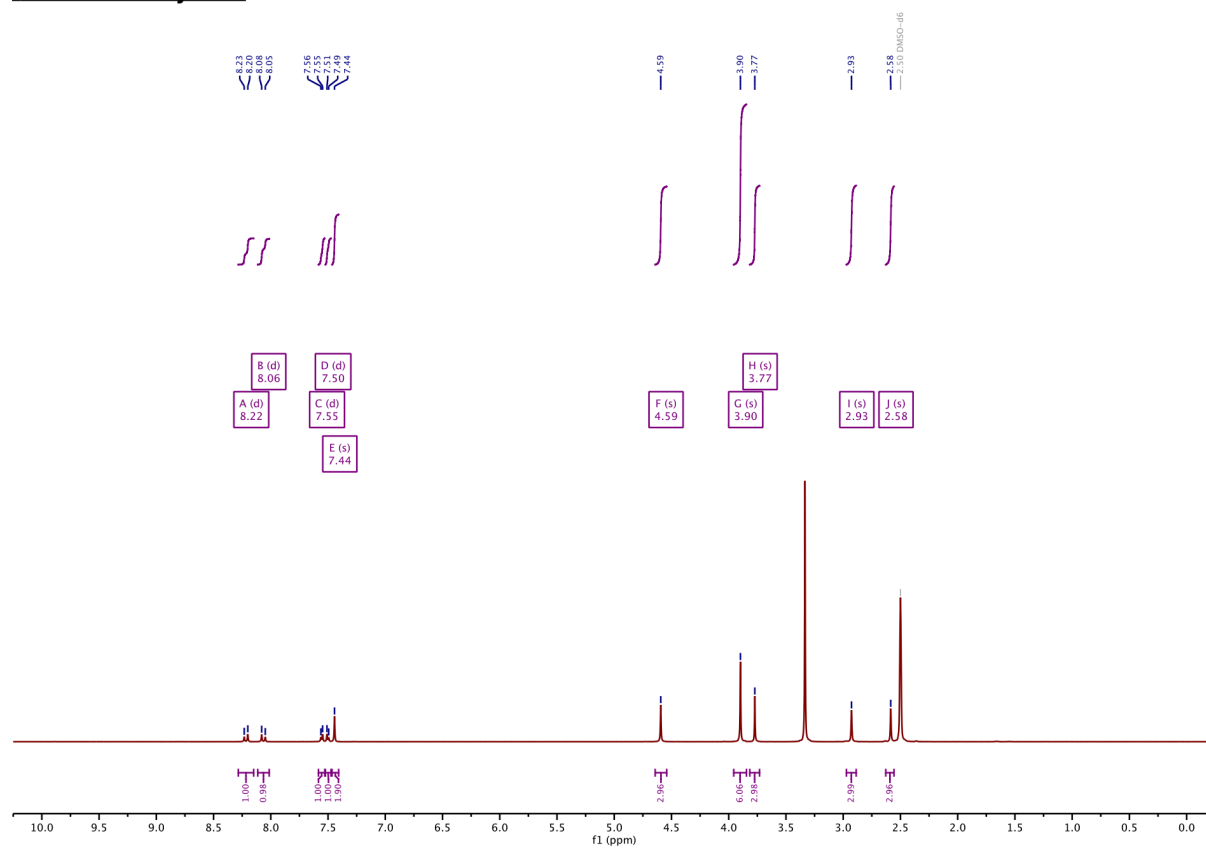
¹H-NMR of StyBtz5



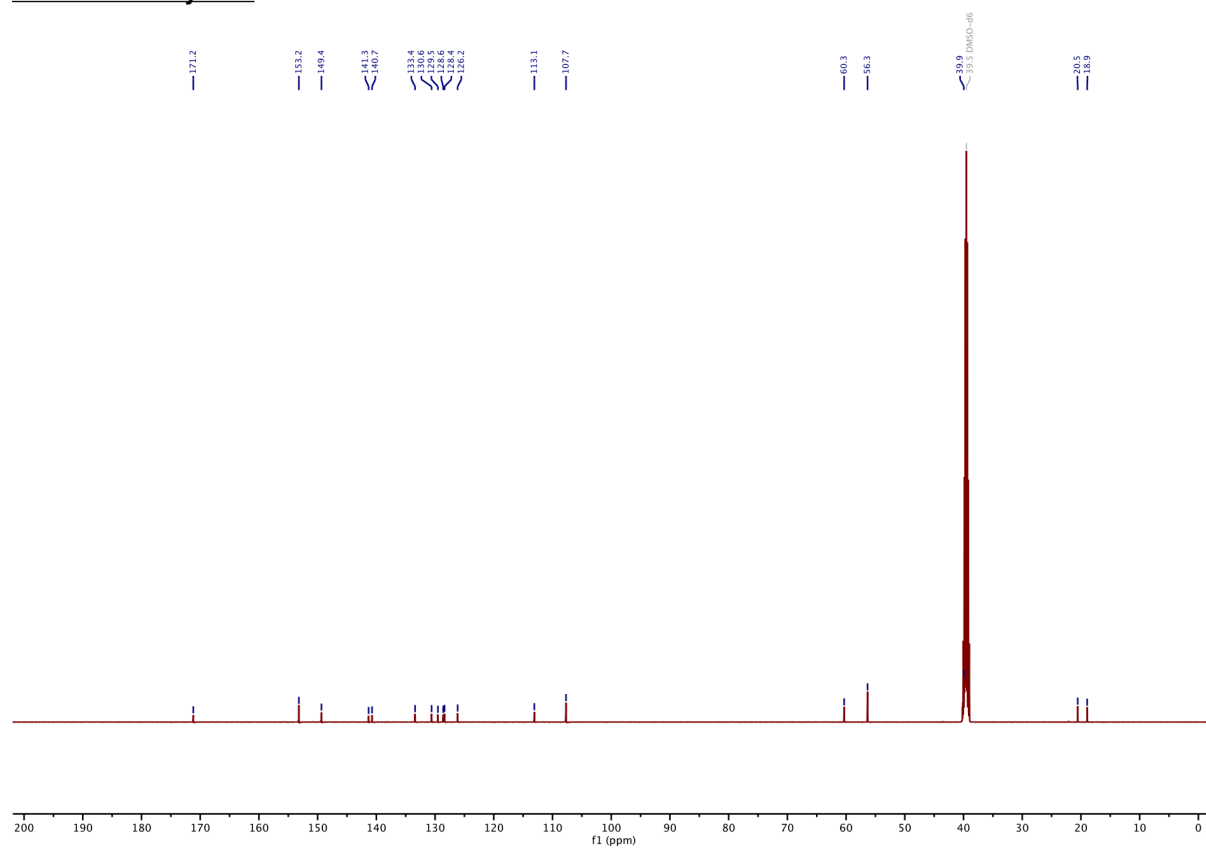
¹³C-NMR of StyBtz5



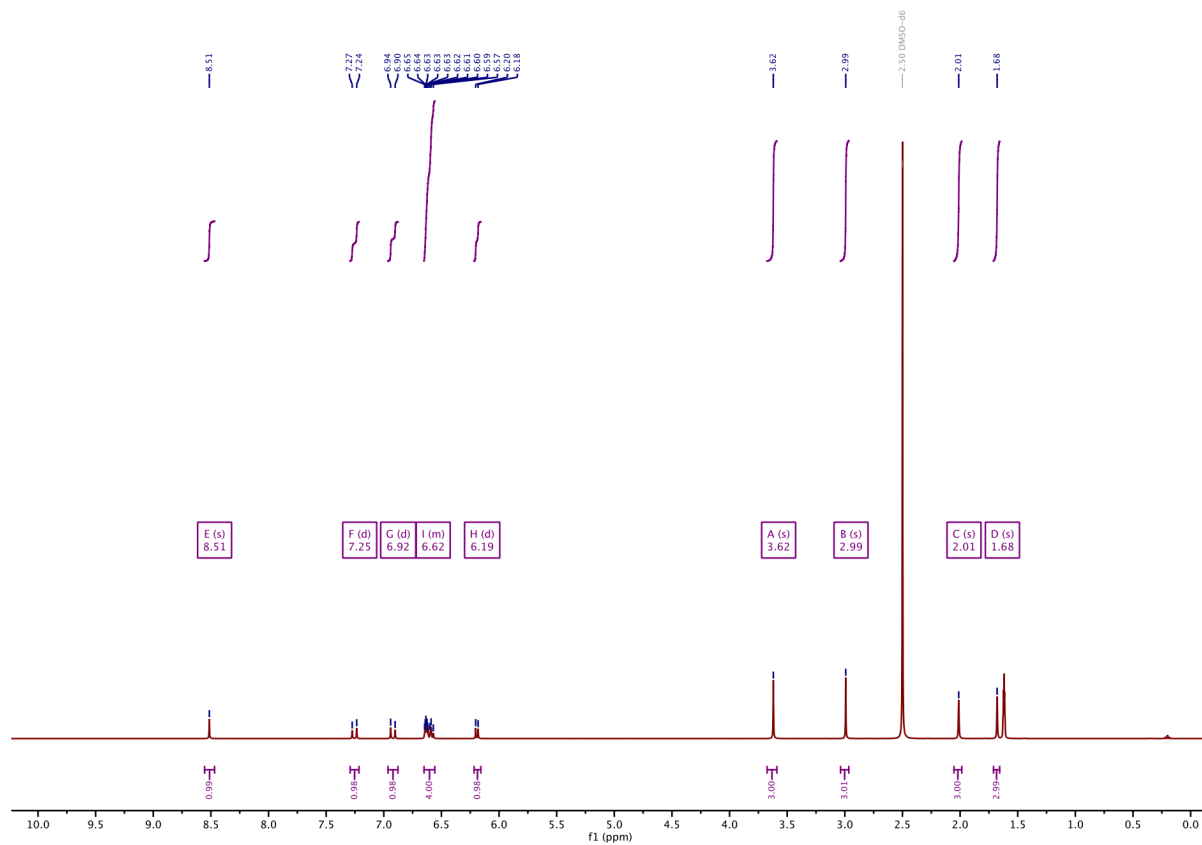
¹H-NMR of StyBtz6



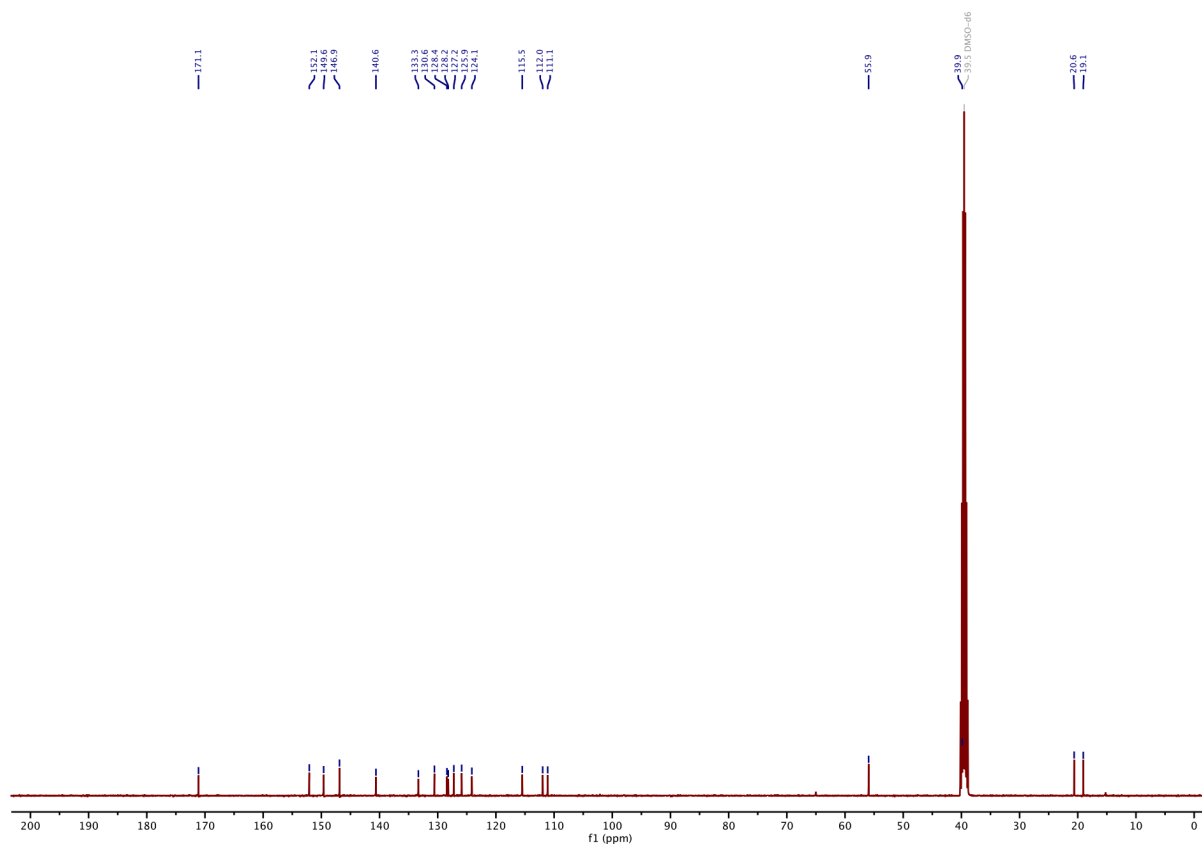
¹³C-NMR of StyBtz6



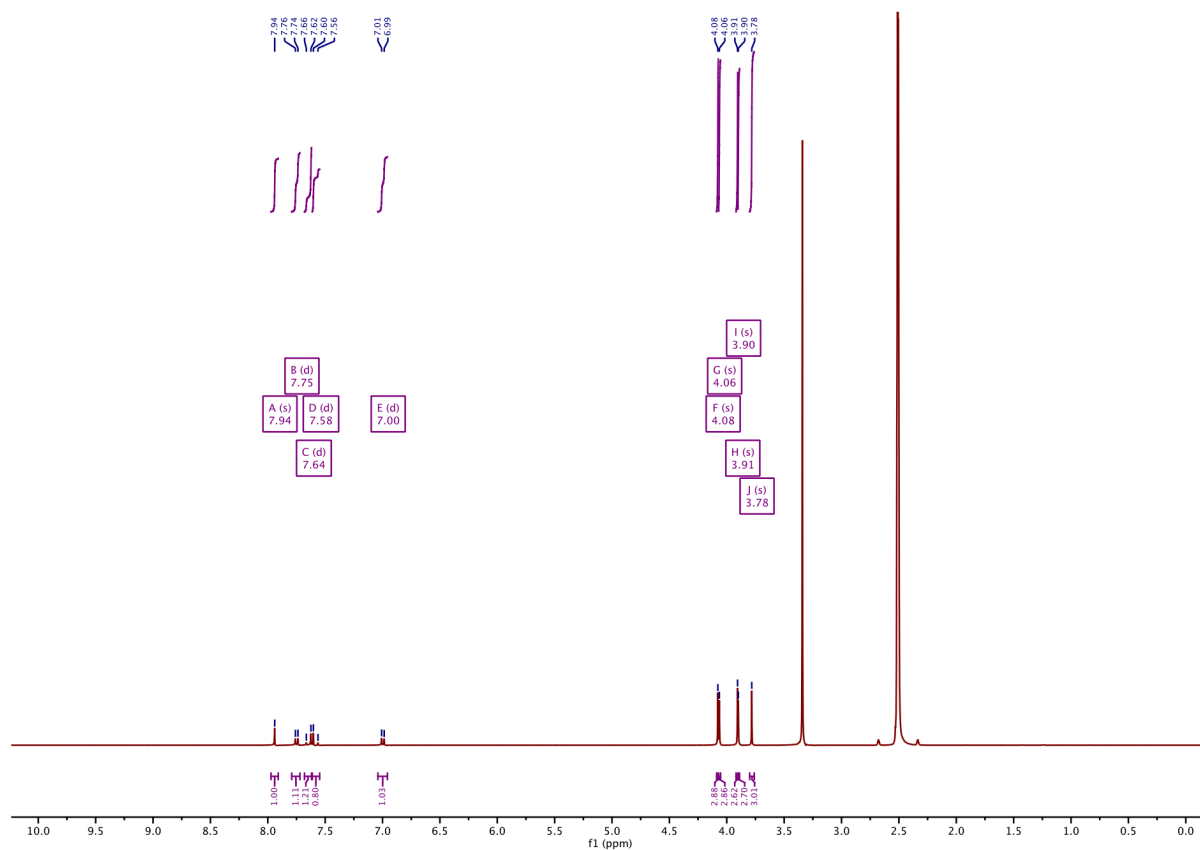
¹H-NMR of StyBtz7



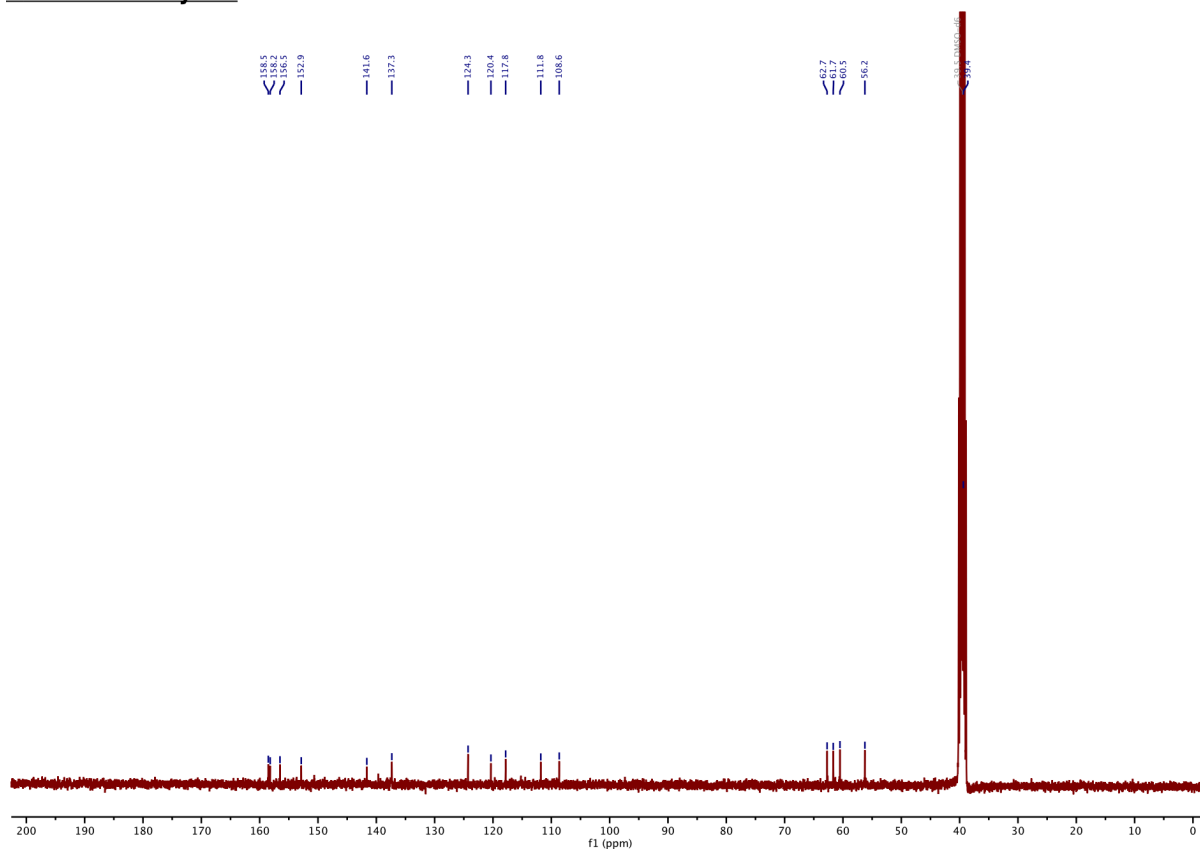
¹³C-NMR of StyBtz7



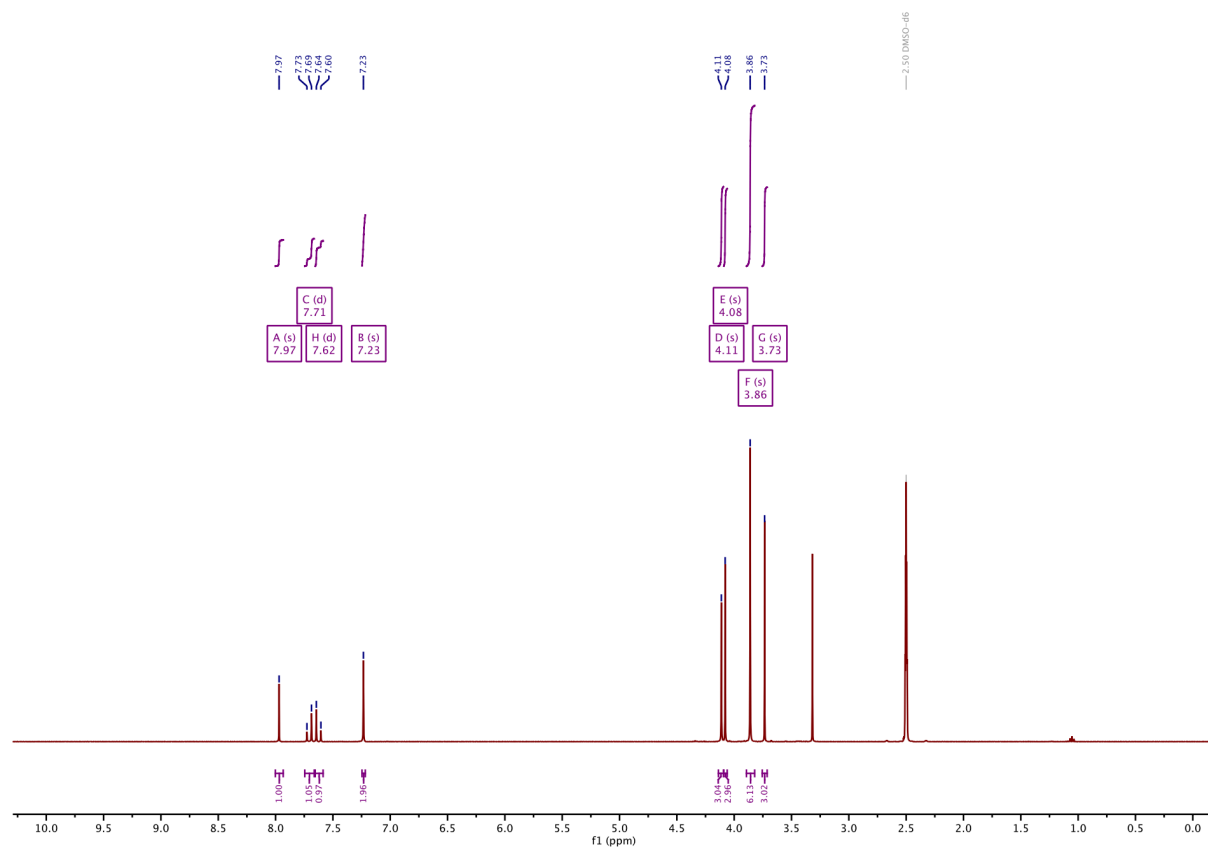
¹H-NMR of StyTz1



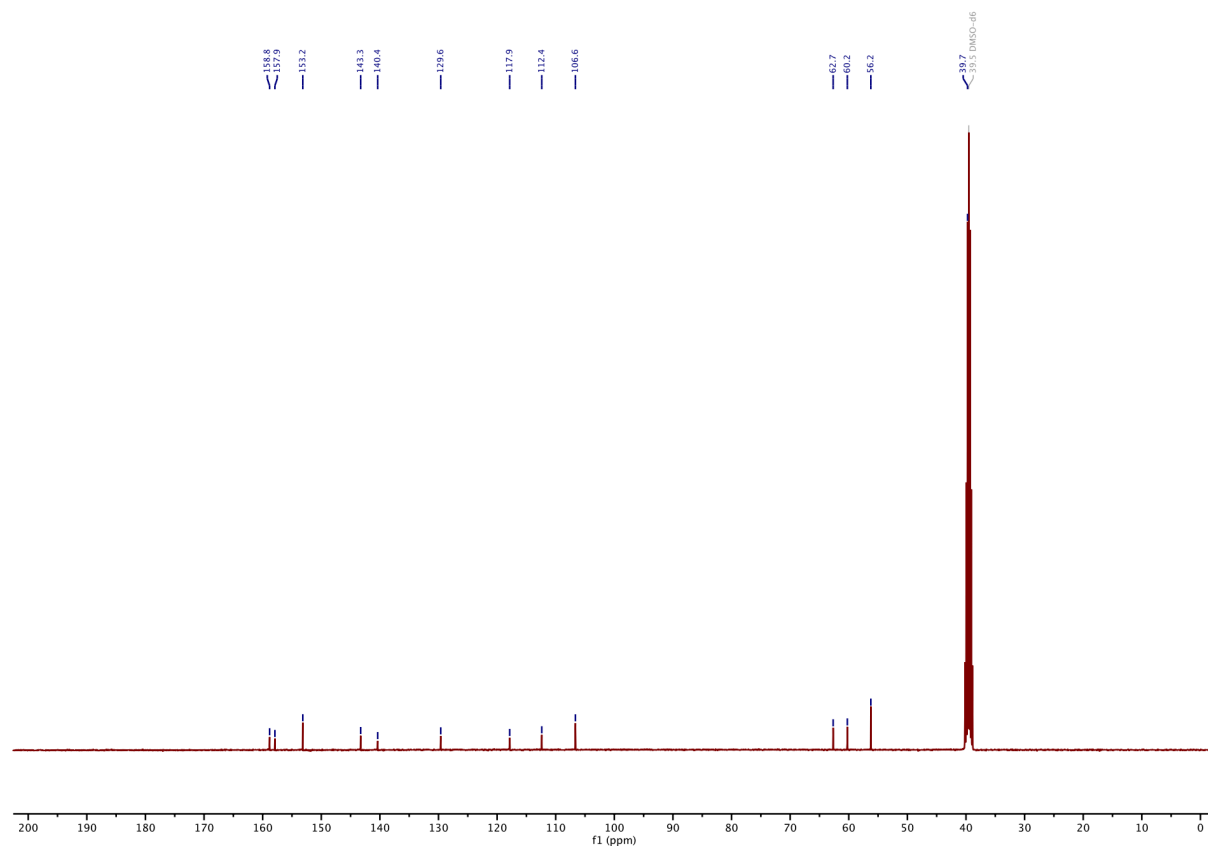
¹³C-NMR of StyTz1



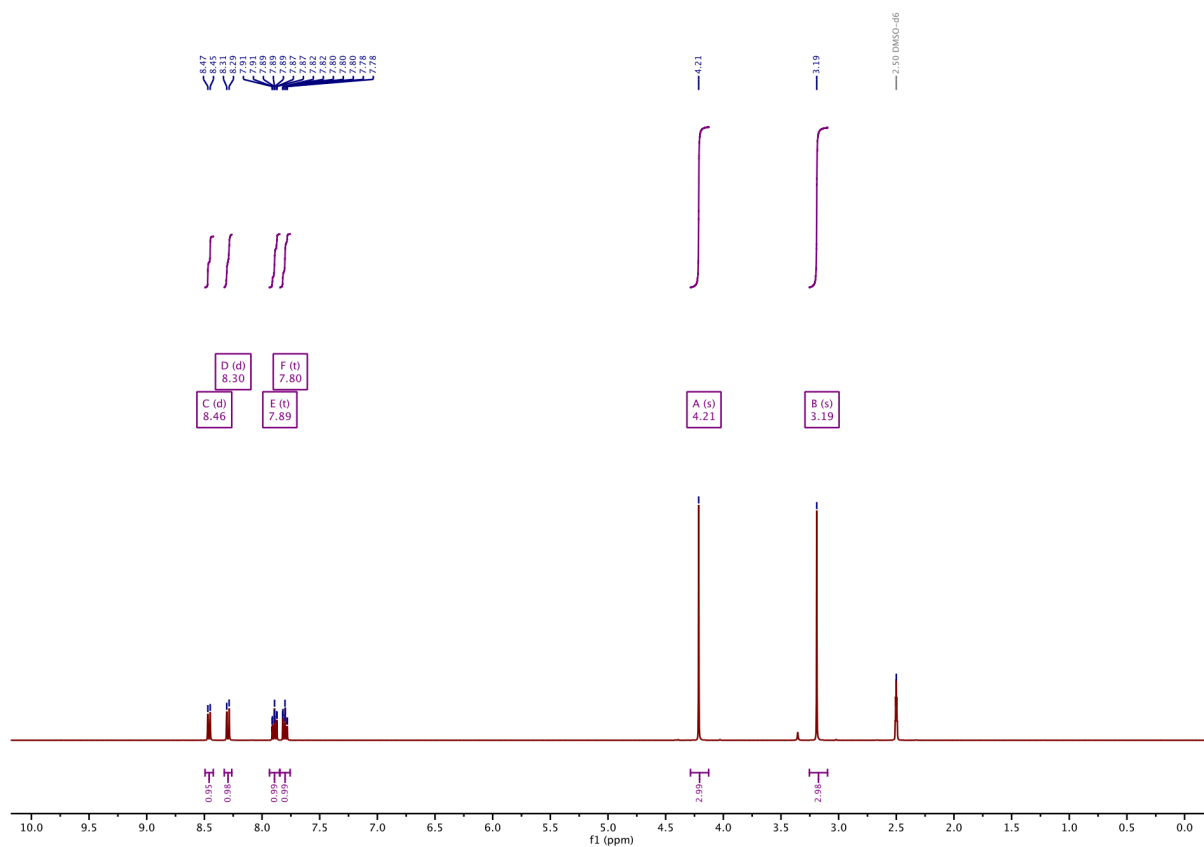
¹H-NMR of StyTz2



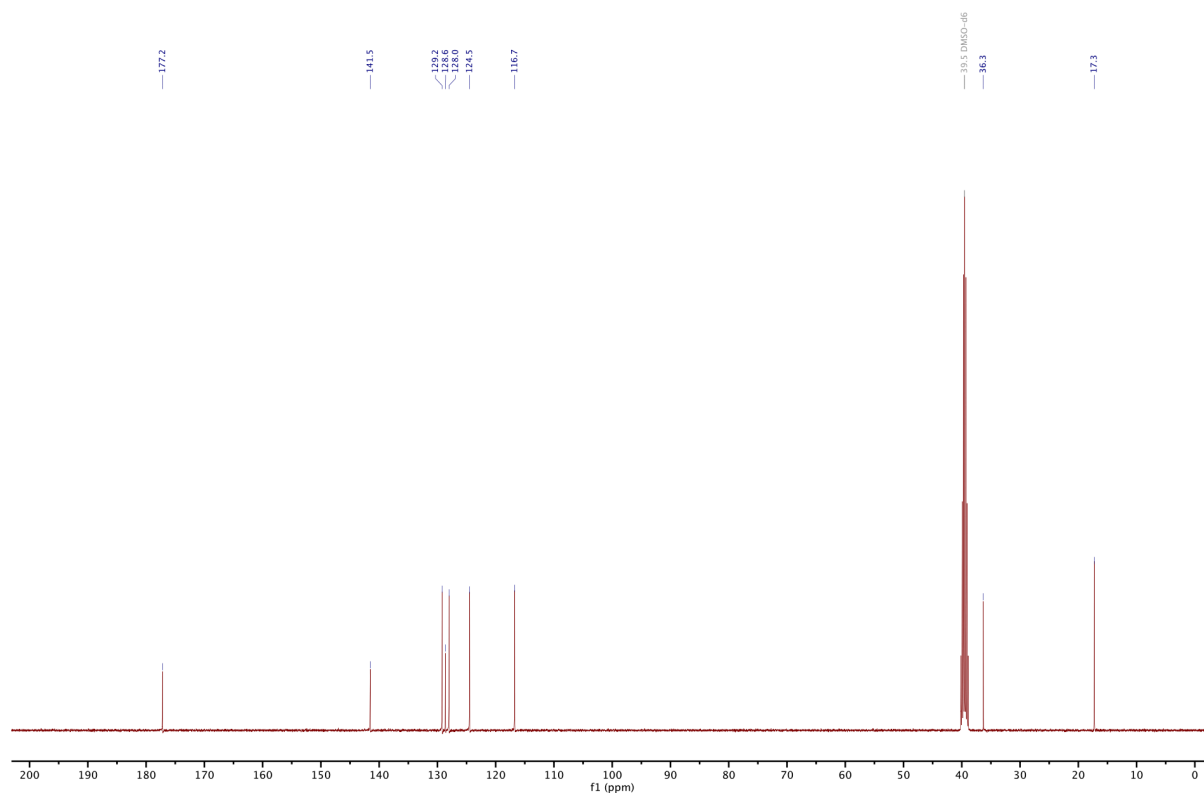
¹³C-NMR of StyTz2



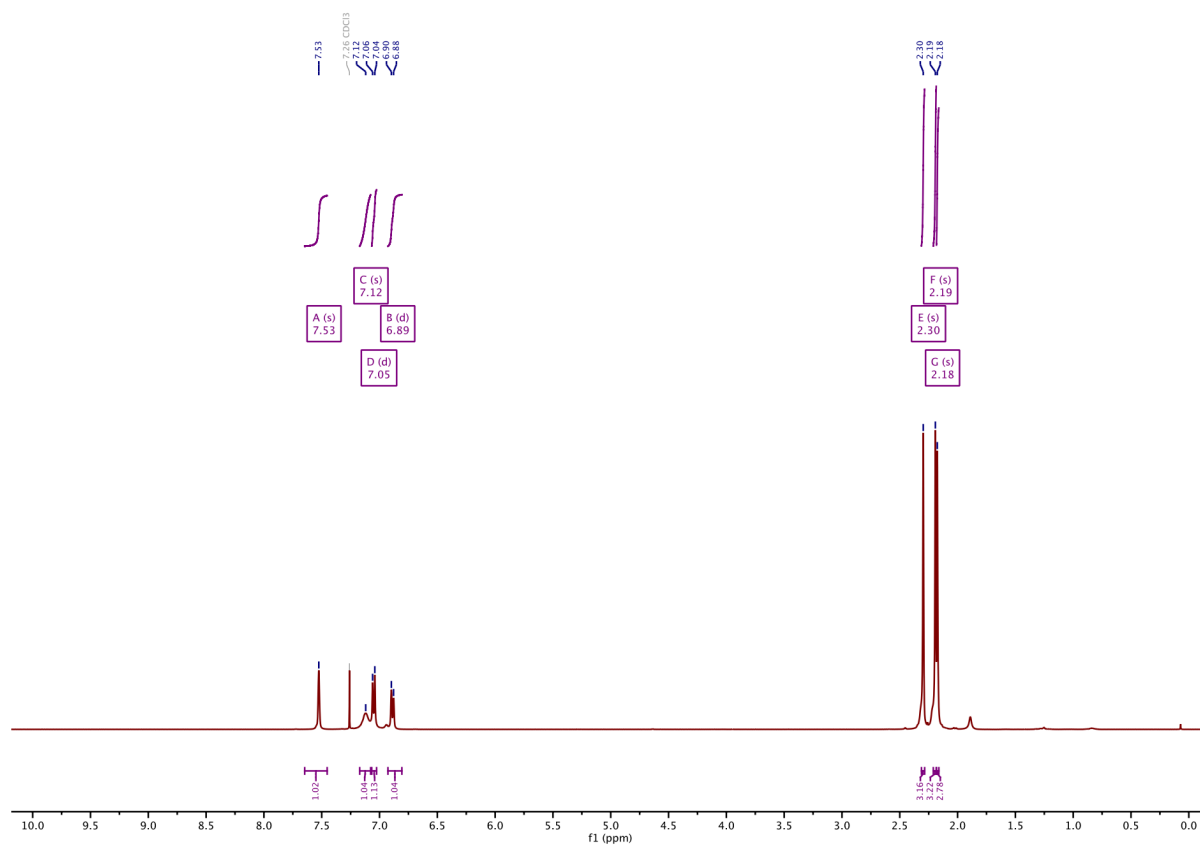
¹H-NMR of 2,3-dimethylbenzothiazolium iodide (1)



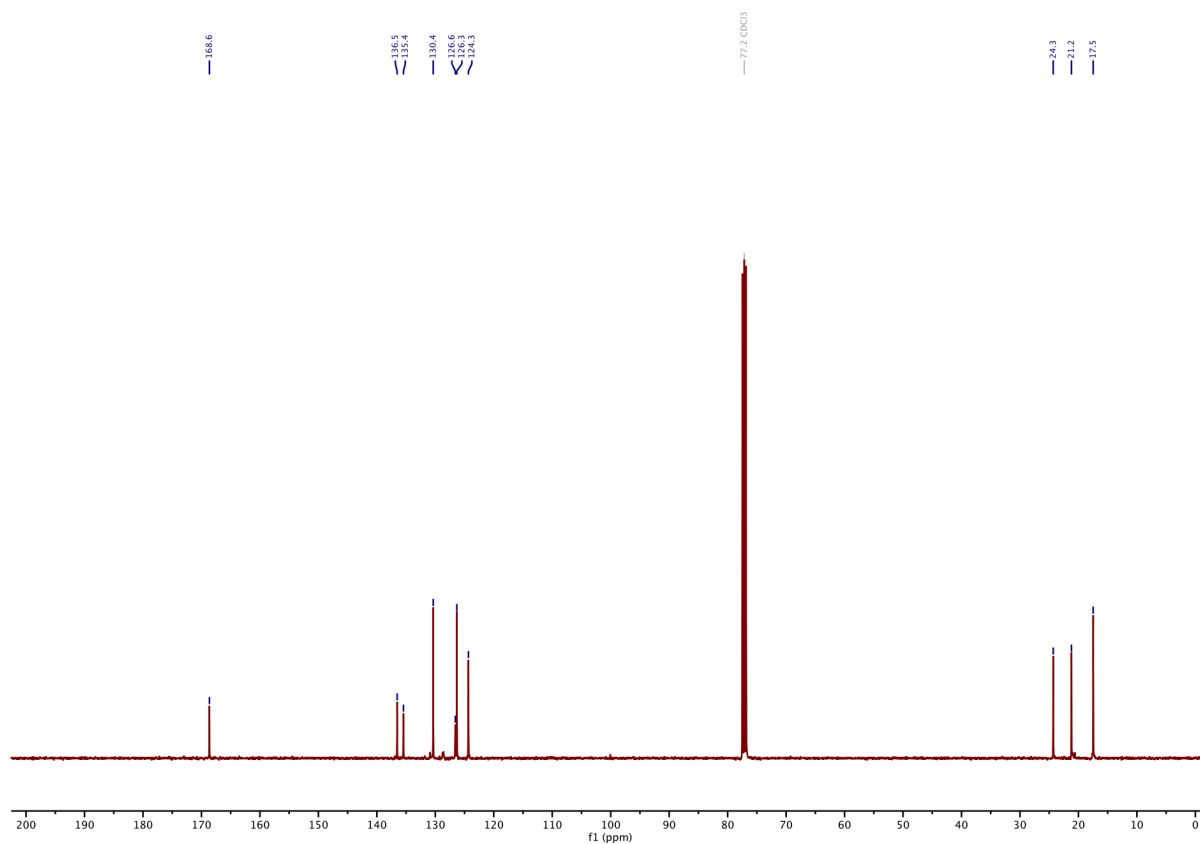
¹³C-NMR of 2,3-dimethylbenzothiazolium iodide (1)



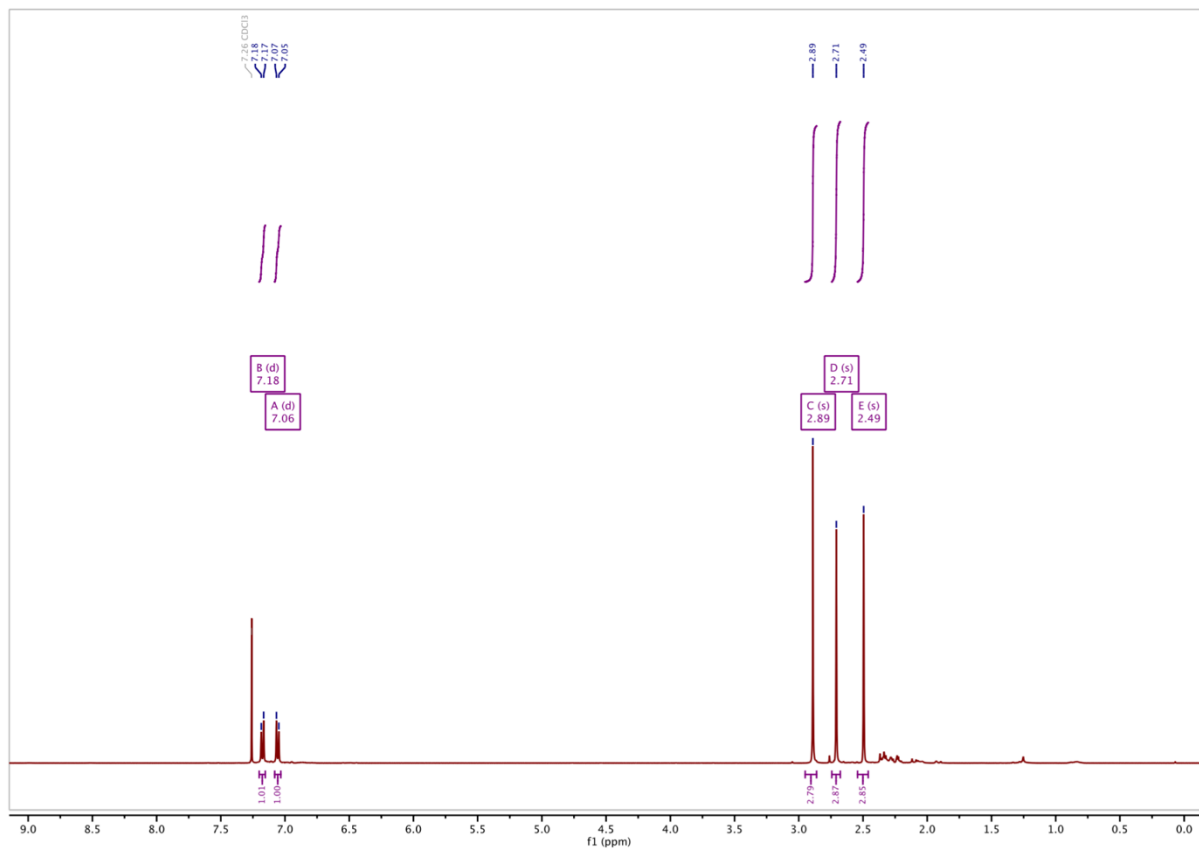
¹H-NMR of Compound 2



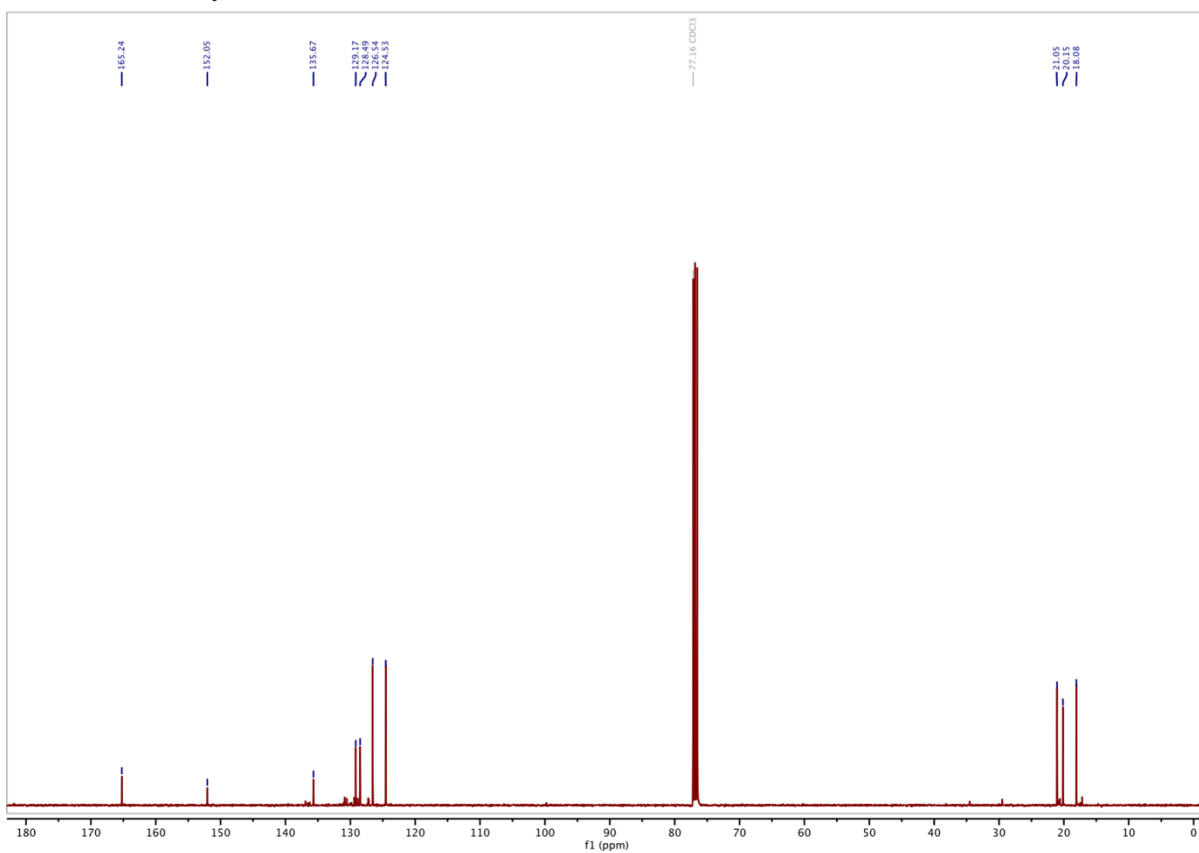
¹³C-NMR of Compound 2



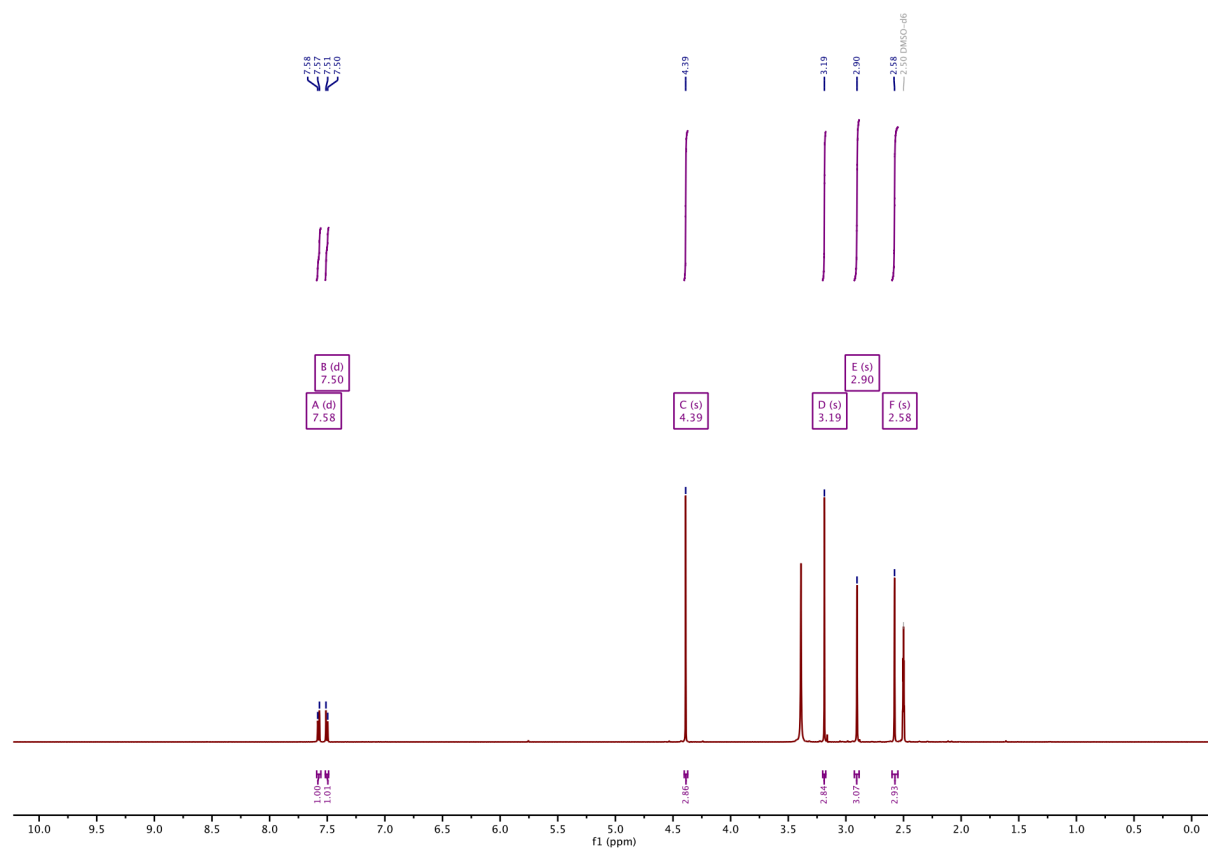
¹H-NMR of Compound 4



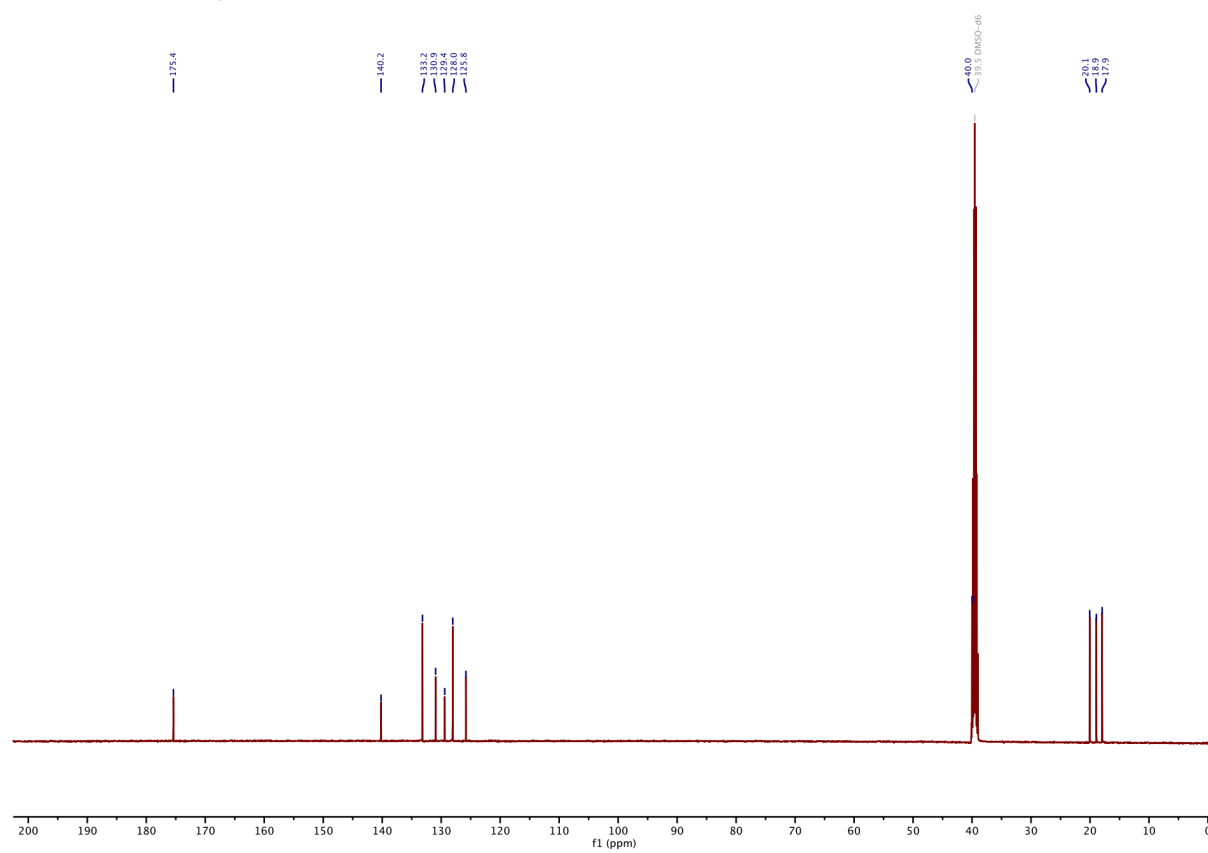
¹³C-NMR of Compound 4



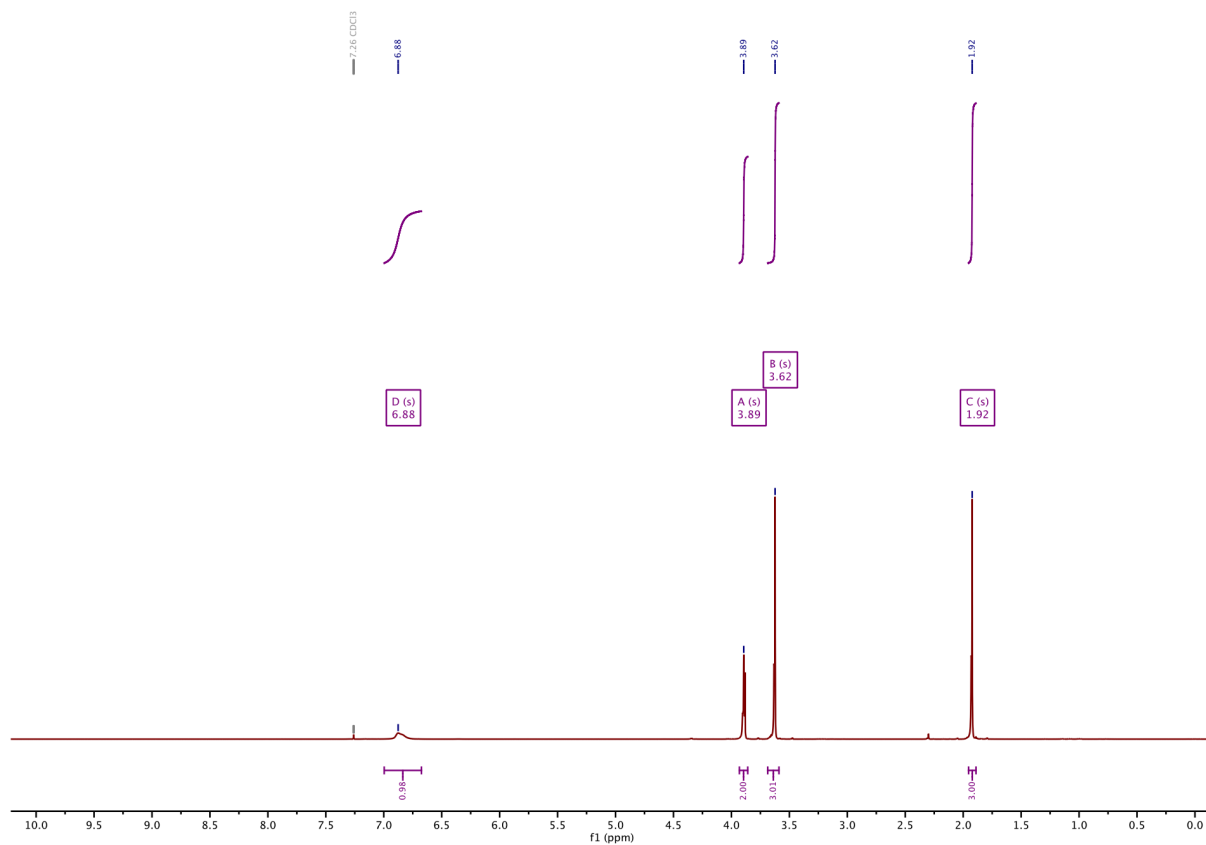
¹H-NMR of Compound 5



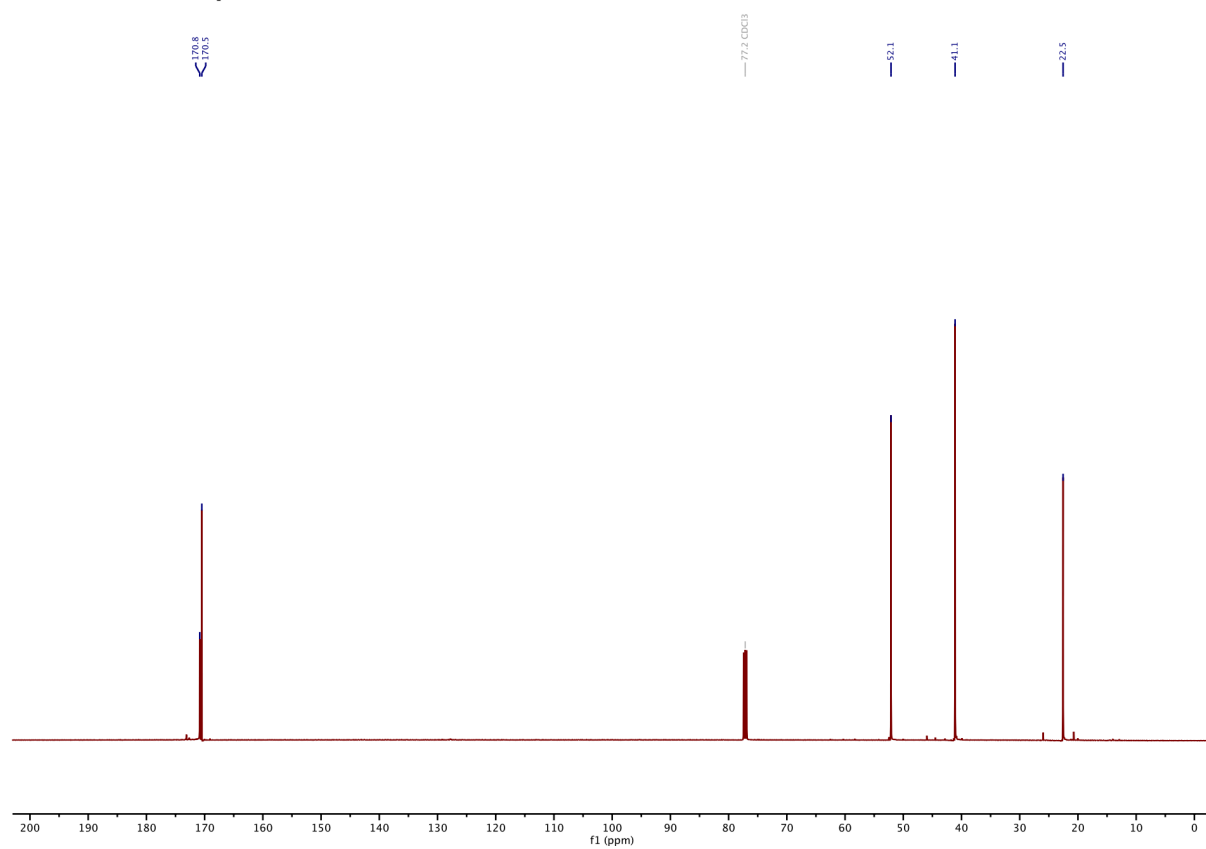
¹³C-NMR of Compound 5



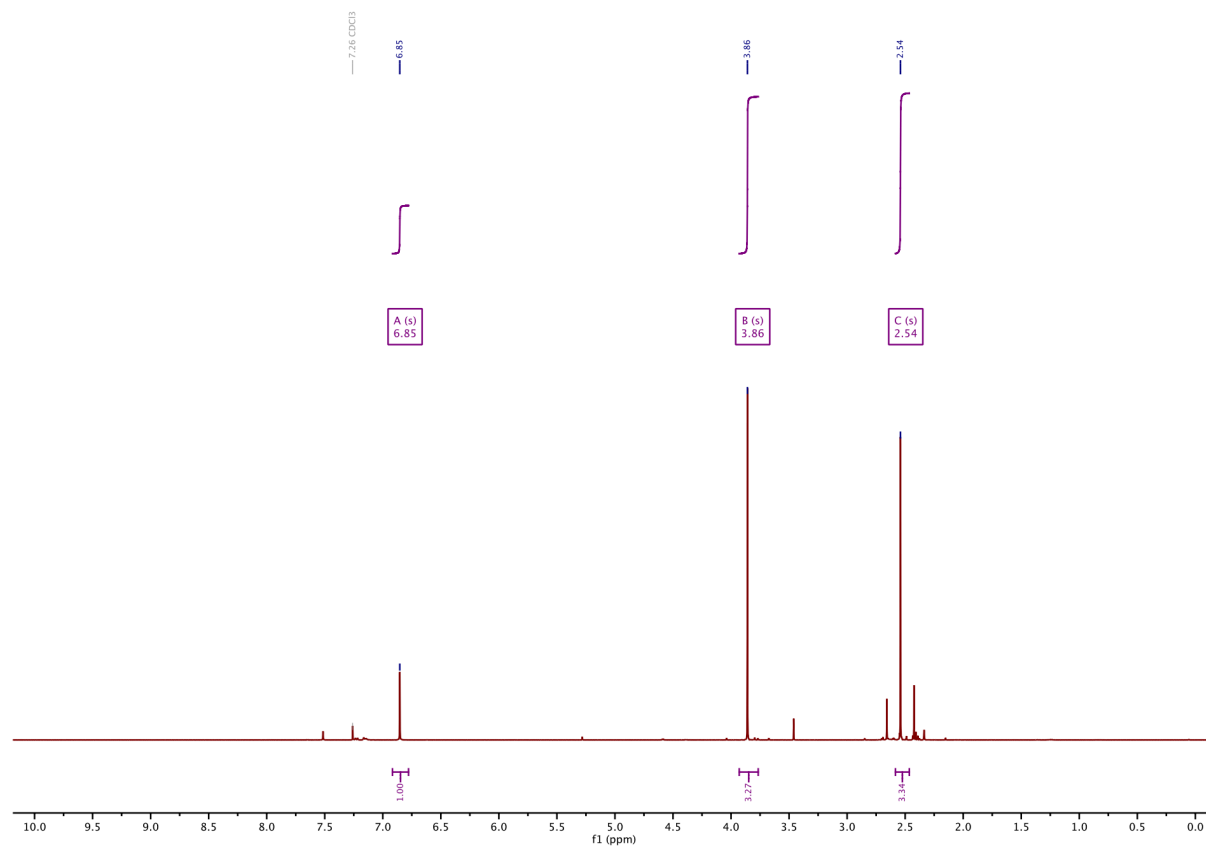
¹H-NMR of Compound 6



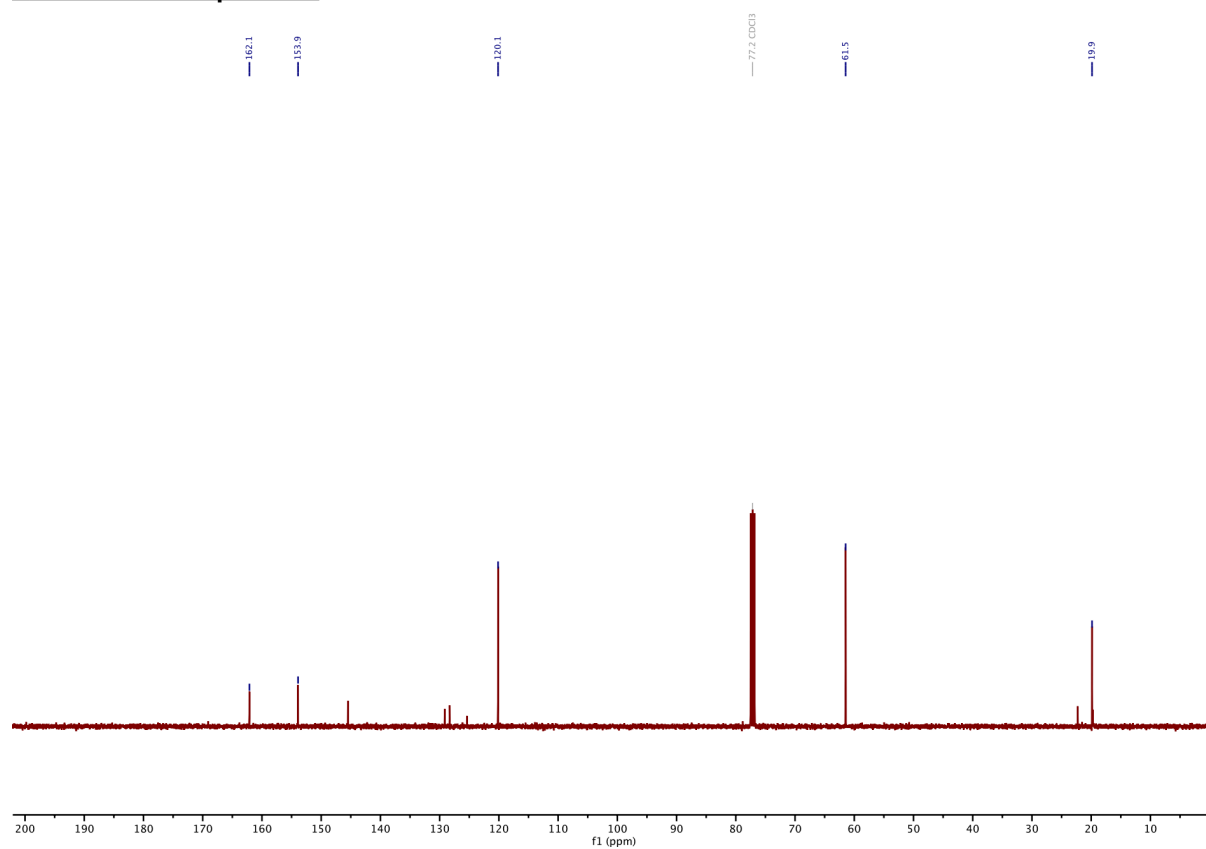
¹³C-NMR of Compound 6



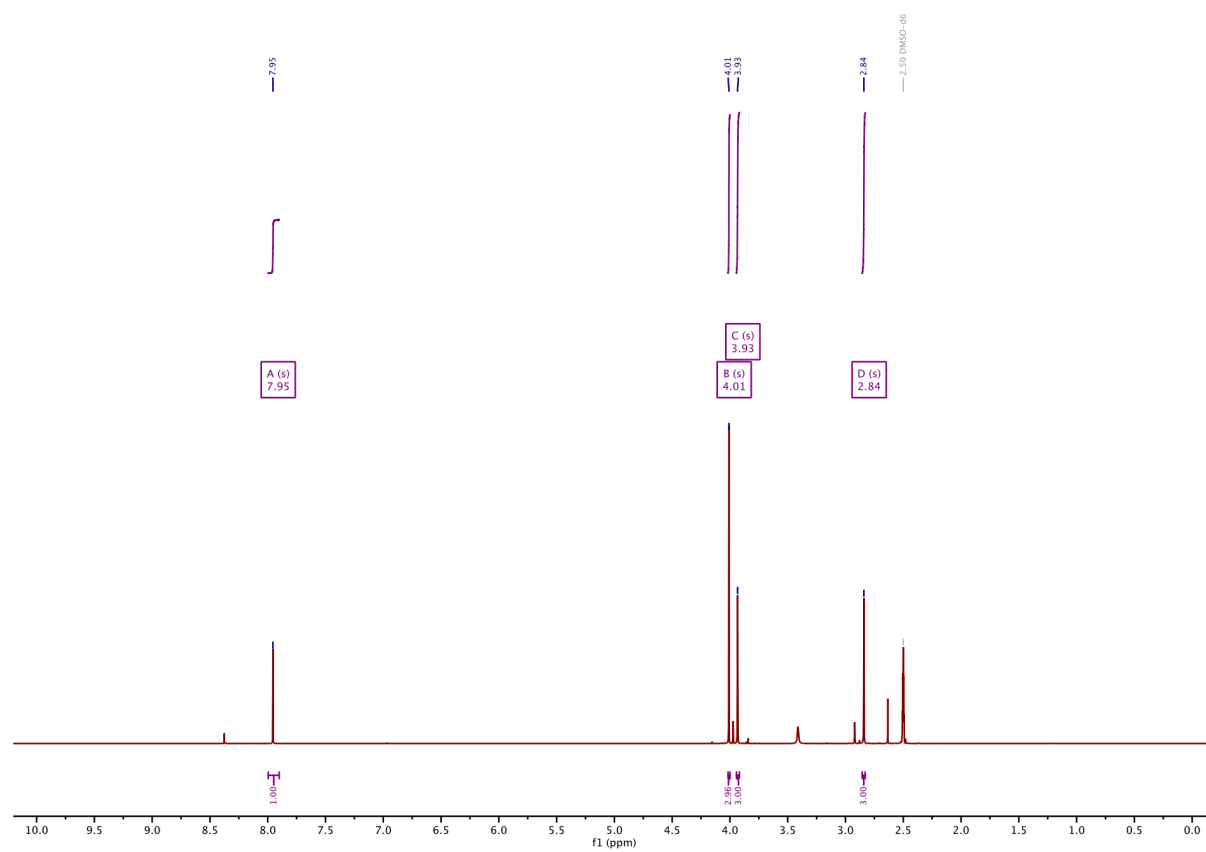
¹H-NMR of Compound 7



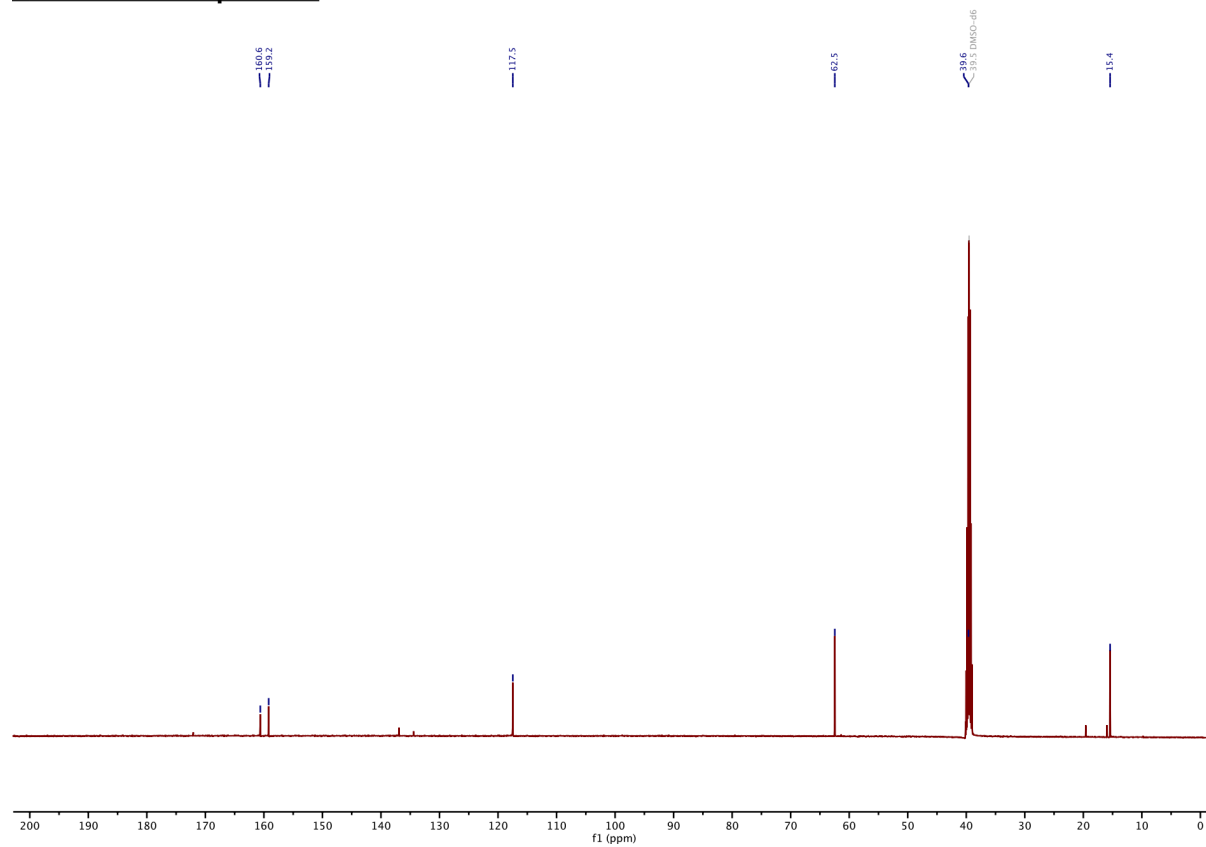
¹³C-NMR of Compound 7



¹H-NMR of Compound 8



¹³C-NMR of Compound 8



Supporting Information References

- [1] M. Borowiak, W. Nahaboo, M. Reynders, K. Nekolla, P. Jalinot, J. Hasserodt, M. Rehberg, M. Delattre, S. Zahler, A. Vollmar, D. Trauner, O. Thorn-Seshold, *Cell* **2015**, *162*, 403–411.
- [2] L. Gao, J. C. M. Meiring, Y. Kraus, M. Wranik, T. Weinert, S. D. Pritzi, R. Bingham, E. Ntoulou, K. I. Jansen, N. Olieric, J. Standfuss, L. C. Kapitein, T. Lohmüller, J. Ahlfeld, A. Akhmanova, M. O. Steinmetz, O. Thorn-Seshold, *Cell Chemical Biology* **2021**, *28*, 228–241.e6.
- [3] G. R. Pettit, S. B. Singh, E. Hamel, C. M. Lin, D. S. Alberts, D. Garcia-Kendal, *Experientia* **1989**, *45*, 209–211.
- [4] R. H. Bisby, S. W. Botchway, J. A. Hadfield, A. T. McGown, A. W. Parker, K. M. Scherer, *European Journal of Cancer* **2012**, *48*, 1896–1903.
- [5] K. M. Scherer, R. H. Bisby, S. W. Botchway, J. A. Hadfield, A. W. Parker, *J. Biomed. Opt.* **2015**, *20*, 051004.
- [6] J. Zenker, M. D. White, R. M. Templin, R. G. Parton, O. Thorn-Seshold, S. Bissiere, N. Plachta, *Science* **2017**, *357*, 925–928.
- [7] J. Zenker, M. D. White, M. Gasnier, Y. D. Alvarez, H. Y. G. Lim, S. Bissiere, M. Biro, N. Plachta, *Cell* **2018**, *173*, 776–791.
- [8] A. Kopf, J. Renkawitz, R. Hauschild, I. Girkontaite, K. Tedford, J. Merrin, O. Thorn-Seshold, D. Trauner, H. Häcker, K.-D. Fischer, E. Kiermaier, M. Sixt, *Journal of Cell Biology* **2020**, *219*, e201907154.
- [9] A. Singh, T. Saha, I. Begemann, A. Ricker, H. Nüsse, O. Thorn-Seshold, J. Klingauf, M. Galic, M. Matis, *Nature Cell Biology* **2018**, *20*, 1126–1133.
- [10] U. Theisen, A. U. Ernst, R. L. S. Heyne, T. P. Ring, O. Thorn-Seshold, R. W. Köster, *Journal of Cell Biology* **2020**, *219*, e201908040.
- [11] L. Gao, J. C. M. Meiring, A. Varady, I. E. Ruider, C. Heise, M. Wranik, C. D. Velasco, J. A. Taylor, B. Terni, T. Weinert, J. Standfuss, C. C. Cabernard, A. Llobet, M. O. Steinmetz, A. R. Bausch, M. Distel, J. Thorn-Seshold, A. Akhmanova, O. Thorn-Seshold, *J. Am. Chem. Soc.* **2022**, *144*, 5614–5628.
- [12] J. Nguyen, A. Tirla, P. Rivera-Fuentes, *Org. Biomol. Chem.* **2021**, *19*, 2681–2687.
- [13] V. García-López, F. Chen, L. G. Nilewski, G. Duret, A. Aliyan, A. B. Kolomeisky, J. T. Robinson, G. Wang, R. Pal, J. M. Tour, *Nature* **2017**, *548*, 567.
- [14] G. R. Fulmer, A. J. Miller, N. H. Sherden, H. E. Gottlieb, A. Nudelman, B. M. Stoltz, J. E. Bercaw, K. I. Goldberg, *Organometallics* **2010**, *29*, 2176–2179.
- [15] P. J. Coelho, M. C. R. Castro, M. M. M. Raposo, *Dyes and Pigments* **2015**, *117*, 163–169.
- [16] D. S. Tarbell, H. P. Hirschler, R. B. Carlin, *J. Am. Chem. Soc.* **1950**, *72*, 3138–3140.
- [17] T.-F. Xuan, Z.-Q. Wang, J. Liu, H.-T. Yu, Q.-W. Lin, W.-M. Chen, J. Lin, *J. Med. Chem.* **2021**, *64*, 11074–11089.
- [18] L. Ma, S. Yang, Y. Ma, Y. Chen, Z. Wang, T. D. James, X. Wang, Z. Wang, *Anal. Chem.* **2021**, *93*, 12617–12627.
- [19] V. Ramesh, B. Ananda Rao, P. Sharma, B. Swarna, D. Thummuni, K. Srinivas, V. G. M. Naidu, V. Jayathirtha Rao, *European Journal of Medicinal Chemistry* **2014**, *83*, 569–580.
- [20] M. Prein, P. J. Manley, A. Padwa, *Tetrahedron* **1997**, *53*, 7777–7794.
- [21] M. M. El-Hendawy, T. A. Fayed, M. K. Awad, N. J. English, S. E. H. Etaiw, A. B. Zaki, *Journal of Photochemistry and Photobiology A: Chemistry* **2015**, *301*, 20–31.
- [22] A. Sailer, J. C. M. Meiring, C. Heise, L. N. Pettersson, A. Akhmanova, J. Thorn-Seshold, O. Thorn-Seshold, *Angewandte Chemie International Edition* **2021**, *60*, 23695–23704.
- [23] A. Müller-Deku, J. C. M. Meiring, K. Loy, Y. Kraus, C. Heise, R. Bingham, K. I. Jansen, X. Qu, F. Bartolini, L. C. Kapitein, A. Akhmanova, J. Ahlfeld, D. Trauner, O. Thorn-Seshold, *Nature Communications* **2020**, *11*, 4640.
- [24] S. Samanta, A. Babalhavaeji, M. Dong, G. A. Woolley, *Angew. Chem. Int. Ed.* **2013**, *52*, 14127–14130.